Heat Shock Factor Regulation of Antimicrobial Peptides Expression Suggests a Conserved Defense Mechanism Induced by Febrile Temperature in Arthropods

Bang Xiao [1, 2], Shihan Chen [1, 2], Yue Wang [1, 2], Xuzheng Liao [1, 2], Jianguo He [1, 2, 3, *], Chaozheng Li [1, 2, 3, **]

1. School of Marine Sciences, Sun Yat-sen University, State Key Laboratory of Biocontrol /Southern Marine Science and Engineering Guangdong Laboratory (Zhuhai), Guangzhou, P. R. China

2. Guangdong Provincial Key Laboratory of Marine Resources and Coastal Engineering/ Guangdong Provincial Key Laboratory for Aquatic Economic Animals, School of Life Sciences, Sun Yat-sen University, Guangzhou, P. R. China

3. China-ASEAN Belt and Road Joint Laboratory on Mariculture Technology, Guangzhou, P. R. China

**, Corresponding Author:
Chaozheng Li, Ph.D.
School of Marine Sciences
Sun Yat-sen University
Guangzhou, 510275
P. R. China
Email: lichaozh@mail2.sysu.edu.cn

*, Corresponding Author:
Jianguo He, Ph.D.
School of Life Sciences
Sun Yat-sen University
Guangzhou, 510275
P. R. China
Email: lsshjg@mail.sysu.edu.cn

Abstract:

Temperature is a critical factor influencing the outbreak and progression of viral diseases in organisms. Febrile temperatures have been shown to enhance immune competence and reduce viral replication in various species. However, the underlying mechanisms remain largely unknown. In this study, we investigate the molecular mechanisms by which elevated temperatures confer resistance to viral infections, focusing on the role of heat shock factor 1 (HSF1) in regulating antimicrobial effectors rather than the traditional target genes molecular chaperones. Using shrimp *Litopenaeus vannamei* as a model, we demonstrate that febrile temperatures induce HSF1, which in turn upregulates antimicrobial peptides (AMPs) that target viral envelope proteins and inhibit viral replication. Importantly, this is the first to show that HSF1 directly binds to the heat shock elements (HSE) motifs of AMPs both in shrimp and *Drosophila*, suggesting this may be a conserved regulatory mechanism in arthropods. Additionally, our findings highlight the role of HSF1 beyond the classical heat shock response, revealing its critical function in modulating innate immunity. These insights provide new avenues for managing viral infections in aquaculture and other settings by leveraging environmental temperature control.

Keywords: Temperature; Innate immunity; Virus; Heat shock factor (HSF); Antimicrobial peptides (AMPs)

1. Introduction

The proliferation of pathogens and the outbreak of diseases are influenced by various factors, including transmission vectors, host species, and environmental conditions (Marcogliese, 2008). Among these, temperature is one of the most critical environmental factors, significantly impacting disease occurrence and prevalence (Hou et al., 2023). Temperature can directly affect the immune response, metabolism, feeding rate, oxygen consumption, growth, and survival of animals (Deldicq et al., 2021). Aquatic animals such as fish, shrimp, crabs, and shellfish are ectothermic, and their susceptibility to diseases is directly related to temperature (Marcogliese, 2008). In fishes, Koi herpesvirus (KHV) can cause massive mortality in carp and koi carp at temperatures between 23-28 °C, while temperatures above 30 °C typically do not result in mortality (Yuasa et al., 2008). In crustaceans, high temperatures (32-33 °C) have been demonstrated to inhibit white spot syndrome virus (WSSV) replication and reduce mortality in infected shrimp (Du et al., 2006; Guan et al., 2003; Jiravanichpaisal et al., 2004). Notably, many ectothermic animals can respond to exogenous pathogenic infections by seeking warmer external environments (Covert and Reynolds, 1977; Louis et al., 1986). When infected, some ectothermic animals such as fish, insects, and crustaceans elevate their body temperature by moving to warmer areas (Bundey et al., 2003; Rakhshaninejad et al., 2023; Rakus et al., 2017). This behavioral fever, similar to fever responses in higher organisms, can help hosts suppress or overcome infections (Hasday et al., 2014), although the mechanisms underlying this heat-induced antimicrobial immunity remain unclear.

The heat shock response (HSR), also known as the heat stress response, serves as a bridge linking elevated temperatures with increased immunity (Evans et al., 2015). The HSR induced by temperature increase primarily involves the expression of heat shock proteins (HSPs) and other related factors regulated by heat shock transcription factors (HSFs) (Barna et al., 2018). Under non-stress conditions, HSF monomers are retained in the cytoplasm in a complex with HSP90 or the cytosolic chaperonin TCP1 ring complex (TRiC) (Neef et al., 2014; Zou et al., 1998). During the stress response, HSF dissociates from the complex, trimerizes, and converts into a DNA-binding

conformation (Zheng et al., 2016). Activated HSF induces gene transcription through regulatory upstream promoter elements known as heat shock elements (HSEs) (Hahn et al., 2004). In the face of thermal or pathogenic stress, the heat shock response functions as a highly conserved cellular mechanism across various organisms (Anckar and Sistonen, 2011). Research suggests that the HSF-mediated heat shock response plays a crucial role in the regulation of the innate immune network through a combination of direct gene regulation, interaction with immune signaling pathways, and the broader cellular stress response (Morimoto, 2011). In *Drosophila*, HSF-deficient flies, lacking a heat shock response, exhibit high sensitivity to viral infection (Merkling et al., 2015), indicating that the heat shock response is a crucial component of innate antiviral immunity.

Heat shock factors (HSFs) are primarily recognized as inducible transcriptional regulators of genes encoding molecular chaperones and other stress proteins (Akerfelt et al., 2010). Interestingly, members of the HSF family also participate in various cellular processes, including apoptosis, the unfolded protein response (UPR), oxidative stress, multidrug resistance, and pathogenic infection (Anckar and Sistonen, 2011). Consequently, the repertoire of HSF targets has expanded well beyond traditional heat shock genes (Barna et al., 2018). Recent research has illuminated the interplay between the heat shock response (HSR) and the innate immune system, revealing that HSFs can regulate innate immune responses (Akerfelt et al., 2007). For instance, HSF1, the primary HSF, can modulate the expression of pro-inflammatory cytokines such as TNF-α, IL-1β, and IL-6, thereby influencing the inflammatory response (Barna et al., 2018). Additionally, HSF1 has been shown to interact with and influence the activity of the NF-κB and MAPK pathways, thus altering the cellular environment to modulate the innate immune response (Chen et al., 2010). These unexpected observations indicate complexity of HSF function. At present, however, the mechanisms by which the HSF family affects innate immunity are still poorly understood.

To explore the underlying mechanisms of the febrile temperature-inducible HSF in host antiviral immunity, the shrimp *Litopenaeus vannamei* was challenged with WSSV, and the thermal regulation of host immunity was characterized. The results

115 indicated that febrile temperature-inducible HSF1 confers virus resistance by regulating
116 the expression of antimicrobial peptides (AMPs) in *L. vannamei*. Additionally, it was
117 revealed that high temperature (30 °C) restricts the replication of *Drosophila* C virus
118 (DCV) in an invertebrate model system (*Drosophila* S2 cells) also mediated by the
119 HSF1-AMPs axis. Together, these results suggest that heat shock factor regulation of
120 AMPs expression is a conserved defense mechanism induced by febrile temperature in
121 arthropods.

2. Results

2.1 Induction of Heat Shock Factor 1 in Response to WSSV at High Temperature (32 °C)

Studies have demonstrated that high temperatures (above 30 °C) markedly reduce mortality in shrimp infected with WSSV, while temperatures ranging from 22 to 30 °C favor higher levels of WSSV replication and associated mortality (Lin et al., 2011; Rahman et al., 2007). To uncover the molecular mechanisms by which high temperature restricts WSSV infection, RNA-seq was performed to identify genes responsive to high temperature, particularly those encoding potential transcriptional regulators. Two shrimp groups, Group TW and Group W, were cultured at 25 °C. Group W comprised shrimp injected with WSSV and maintained at 25 °C continuously. In contrast, Group TW was subjected to a temperature increase to 32 °C at 24 hours post-injection (hpi). Gill samples were collected for analysis 12 hours post-temperature rise (hptr) and subjected to Illumina sequencing (Fig. 1A). As shown in Fig. 1B and 1C, 10 of the 1285 high temperature-induced genes were predicted to encode transcription factors.

Special attention has been paid to heat shock factor 1 (HSF1), the master regulator of the heat shock response, which upon activation induces not only classical heat shock genes but also a broad array of genes beyond the scope of molecular chaperones (Barna et al., 2018). To validate the high-throughput sequencing results, the expression profile of these transcription factors was confirmed by qPCR, showing a significant increase in LvHSF1 expression (Supplementary Fig. 1). These results suggest that LvHSF1 may play a key role in enhancing shrimp resistance to WSSV at elevated temperatures (32 °C).

2.2 Expression Profiles of LvHSF1 in Shrimp Under Varied Temperature Conditions and WSSV Challenge

To determine that LvHSF1 is related to high temperature and WSSV infection, its expression level was measured under high temperature and after WSSV infection. Tissue distribution analysis showed that LvHSF1 was expressed in all examined tissues at room temperature (25 °C) and increased rapidly in all tested tissues at high temperature (32 °C; Fig. 2A). Additionally, the protein expression of LvHSF1 was

152 significantly up-regulated in hemocytes, gills, and intestines when exposed to 32 °C
153 (Fig. 2B). Further investigation revealed LvHSF1's role in the immune response to Poly
154 (I:C) and WSSV at 25 °C. Following exposure to Poly (I:C), LvHSF1 expression was
155 upregulated at 12 h (2.43-fold), 24 h (2.60-fold), and 36 h (4.33-fold) in hemocytes (Fig.
156 2C); slightly upregulated at 4 h (1.97-fold) and downregulated at 12 h (0.64-fold) in
157 gills (Fig. 2D); and slightly downregulated at 4 h (0.41-fold) and upregulated at 8 h
158 (1.15-fold) in intestines (Fig. 2E). In response to WSSV infection, LvHSF1 expression
159 in hemocytes was dramatically induced, peaking at 8 hours (6.04-fold; Fig. 2F). In the
160 gills, LvHSF1 expression initially increased at 8 hours (2.10-fold) and significantly
161 again at 72 hours (2.80-fold; Fig. 2G). In the intestines, a marked induction of LvHSF1
162 was observed at 8 hours (2.23-fold; Fig. 2H). These results suggest that LvHSF1 is
163 actively involved in the response to both elevated temperatures and viral (WSSV)
164 infection.

165 **2.3 Role of LvHSF1 in Restricting WSSV at Low (25 °C) and High (32 °C)**
166 **Temperatures**

167 To investigate LvHSF1's role in shrimp during WSSV infection, RNA interference
168 (RNAi) was employed *in vivo*. Two dsLvHSF1 constructs were synthesized:
169 dsLvHSF1-1 (targeting 443-1001 bp) and dsLvHSF1-2 (targeting 1365-1854 bp).
170 Analysis revealed a significant reduction in both transcription and protein levels of
171 LvHSF1 in hemocytes (Figs. 3A, 3a) and gills (Figs. 3B, 3b), with dsLvHSF1-1
172 showing greater silencing efficiency. Consequently, dsLvHSF1-1 was selected for
173 subsequent knockdown experiments. After LvHSF1 knockdown, shrimp were
174 challenged with WSSV, and viral titers were quantified using absolute quantitative PCR.
175 Shrimp with silenced LvHSF1 exhibited increased viral loads in hemocytes (Fig. 3C)
176 and gills (Fig. 3D) at low temperature (25 °C). Additionally, transcription levels of
177 VP28, one of the major structural proteins of WSSV, were higher in the LvHSF1-
178 silenced group than in the GFP-silenced control in hemocytes (Fig. 3E) and gills (Fig.
179 3F). Similarly, the levels of VP28 protein were significantly elevated in the HSF1-
180 silenced group (Figs. 3G, 3g). However, no significant difference in shrimp survival

181 rates was observed between LvHSF1-silenced shrimp and GFP-silenced shrimp at low
182 temperature (25 °C) ($p = 0.8657$; Fig. 3H).
183 Next, LvHSF1's role in shrimp during WSSV infection at high temperature (32 °C)
184 was further determined. Notably, the survival rate of LvHSF1-silenced shrimp infected
185 with WSSV was significantly lower than the control group at high temperature (32 °C)
186 ($p < 0.001$; Fig. 4A). Shrimp with silenced LvHSF1 exhibited increased viral loads in
187 gills (Fig. 4B) and muscle (Fig. 4C) at high temperature (32 °C). Additionally, VP28
188 protein levels were significantly elevated in the LvHSF1-silenced group in gills at high
189 temperature (32 °C; Figs. 4D, 4d). These data suggest that LvHSF1 plays a crucial role
190 in antiviral immunity against WSSV infection especially at high (32 °C) temperatures.
191 **2.4 nSWD as a Potential Antiviral Effector Regulated by LvHSF1**
192 To determine how temperature-induced LvHSF1 restricts WSSV infection, RNA-
193 seq was performed to identify target genes regulated by LvHSF1. Candidates whose
194 expression was inhibited by LvHSF1 knockdown after WSSV infection at high
195 temperature (32 °C) were screened. As shown in Fig. 5A and 5B, 8 of the 954 dsHSF1-
196 suppressed genes were predicted to encode effector factors. These differentially
197 expressed genes (DEGs) included immunity-effector molecules, such as antimicrobial
198 peptides and cytokines. Among the 8 candidate genes, particular attention was paid to
199 the **n**ewly identified **s**ingle **w**hey acidic protein **d**omain-containing protein, designated
200 nSWD. The nSWD belongs to type III crustins, which are crustacean cationic cysteine-
201 rich antimicrobial peptides containing one or two whey acidic protein (WAP) domains
202 at the carboxyl terminus and mainly exert antimicrobial activities. The detailed
203 regulatory mechanism of nSWD against WSSV was unclear. To validate the high-
204 throughput sequencing results, the expression level of nSWD and effector molecules
205 were confirmed by qPC, showing a significant reduction in hemocytes and gills after
206 LvHSF1-knockdown (Fig. 5C; Supplementary Fig. 2). These results suggest that
207 nSWD may play a pivotal role against WSSV infection regulated by LvHSF1.
208 To determine whether LvHSF1 regulates the expression of nSWD *in vitro*, a dual-
209 luciferase reporter assay was performed in *Drosophila* S2 cells. The promoter region of
210 nSWD was cloned by genome walking, containing two putative conserved HSE motifs

211 located at approximately −1371 to −1359 (HSE-1) and −1035 to −1023 (HSE-2;
212 Supplementary data). The dual-luciferase reporter assay showed that the promoter of
213 nSWD could be regulated by ectopic expression of LvHSF1 in a dose-dependent
214 manner (Figs. 5D and 5d). Three reporter plasmids containing mutant promoter regions
215 of nSWD with one or no HSE motifs were constructed, named pGL3-nSWD-M1,
216 pGL3-nSWD-M2, and pGL3-nSWD-M12, respectively (Fig. 5E). The reporter assay
217 results showed that the ectopic expression of LvHSF1 could also improve the promoter
218 activity of pGL3-nSWD-M1 and pGL3-nSWD-M2, whereas the activity of pGL3-
219 nSWD-M12 was not upregulated (Figs. 5F and 5f), suggesting that putative HSE
220 binding motifs play significant roles in LvHSF1-mediated nSWD induction.

221 To further confirm this, EMSA experiments were performed to investigate the
222 direct interaction between LvHSF1 and HSE motifs of nSWD. Biotin-labeled probes
223 or mutant probes of the HSE motifs were synthesized (Fig. 5G). LvHSF1 protein was
224 purified to verify its ability to bind to the HSE motifs (Supplementary Fig. 3A and 3B).
225 The results showed that band shifts of protein-DNA complexes were detected when
226 LvHSF1 protein was incubated with biotin-labeled probe1 but not mutant biotin-labeled
227 probe1 (Fig. 5H). Additionally, the band shifts could be competitively reduced when
228 LvHSF1 protein was incubated with wide-type unbiotinylated probe1 at 20- and 100-
229 fold molar excess (Fig. 5H). A similar result was observed in the interaction between
230 LvHSF1 protein and the biotin-labeled probe2 (Fig. 5H). No band shift was observed
231 in the control set (GST), suggesting that the interaction between LvHSF1 protein and
232 each of the HSE binding motifs is specific. These results strongly demonstrate that
233 LvHSF1 could regulate the expression of nSWD *in vitro* and *in vivo*.

234 **2.5 nSWD Inhibits WSSV Replication and Interacts with WSSV Envelope Proteins**

235 To confirm whether nSWD is involved in WSSV infection, qPCR was performed
236 to determine the expression profile of nSWD. When shrimp were infected with WSSV,
237 the expression of nSWD was upregulated at 4 h (5.66-fold) and 12 h (5.60-fold),
238 remained high at 36 h (5.18-fold) and 48 h (7.90-fold), and slightly downregulated at
239 72 h (4.74-fold; Fig. 6A). To reveal the role of nSWD in WSSV infection at high
240 temperature (32 °C), RNA interference (RNAi) was performed to knock down nSWD

241 expression. The mRNA level of nSWD was effectively suppressed by specific dsnSWD
242 in gills, and the value was downregulated to 0.30-fold of the dsGFP (green fluorescent
243 protein) injection group (as a control) (Fig. 6B). The viral load of the dsnSWD group
244 was considerably higher than the control group (Fig. 6C). Additionally, the survival rate
245 of shrimp in the nSWD-silenced group was significantly lower than in the GFP-
246 knockdown group ($p < 0.01$; Fig. 6D).

247 To further demonstrate the actual role of nSWD *in vivo*, RNAi experiments coupled
248 with rnSWD proteins injection were performed. Recombinant proteins of rnSWD and
249 rTrx-His-tag were expressed, purified by SDS-PAGE gels, and confirmed by
250 Coomassie staining (Fig. 6E), and the results were further confirmed by Western blot
251 analysis (Fig. 6F). After knockdown of endogenous nSWD, shrimp samples were
252 treated with WSSV mixed with rnSWD or rTrx-His-tag by intramuscular injection at
253 high temperature (32 °C). Consequently, the viral load of those co-injected with rnSWD
254 was significantly reduced compared to the control group ($p < 0.01$; Fig. 6G).
255 Additionally, the survival rates of shrimp co-injected with rnSWD were significantly
256 higher than the control group ($p < 0.01$; Fig. 6H). Therefore, nSWD plays a crucial role
257 in the immune defense against WSSV infection at high temperature (32 °C) *in vivo*.

258 Next, to verify whether the anti-WSSV function of nSWD was mediated by
259 LvHSF1 at high temperature (32 °C), *in vivo* RNAi-LvHSF1 experiments coupled with
260 rnSWD injection were performed. After knockdown of LvHSF1, shrimp samples were
261 treated with WSSV mixed with rnSWD or rTrx-His-tag by intramuscular injection at
262 high temperature (32 °C). The results showed that the viral load of those co-injected
263 with rnSWD was significantly reduced compared to the control group ($p < 0.01$; Fig.
264 6I). Additionally, VP28 protein levels of those co-injected with rnSWD were
265 significantly decreased (Fig. 6J, 6j). The survival rates of shrimp co-injected with
266 rnSWD were significantly higher than the control group ($p < 0.01$; Fig. 6K). These
267 results suggest that the anti-WSSV function of nSWD at high temperature (32 °C) is
268 mediated by LvHSF1.

269 To reveal the possible anti-WSSV mechanism of nSWD, pull-down assays were
270 performed to detect whether rnSWD protein could interact with WSSV envelope

271 proteins. The main envelope proteins of WSSV, including VP19, VP24, VP26, and
272 VP28 with GST-tags, were from a previous study. In the GST-tagged pull-down assays,
273 rnSWD could interact with VP24 and VP26 based on SDS-PAGE gels with Coomassie
274 blue staining (Fig. 7A), and the result was further confirmed by Western blot analysis
275 with the 6×His antibody (Fig. 7B). Based on the His-tagged pull-down assays, VP24
276 and VP26 could precipitate rnSWD (Fig. 7C), and this result was further confirmed by
277 Western blot analysis with GST antibody (Fig. 7D). Additionally, confocal analysis
278 confirmed that nSWD colocalized with VP24 (Fig. 7E and 7e) and VP26 (Fig. 7F and
279 7f) in *Drosophila* S2 cells. Collectively, these results suggest that nSWD could inhibit
280 WSSV replication and bind to VP24 and VP26 of WSSV.

281 **2.6 Conservation of the Febrile Temperature-Inducible HSF1-AMPs Axis**
282 **Conferring Virus Resistance in Arthropods**

283 To demonstrate whether HSF1 regulation of antimicrobial peptides is a conserved
284 defense mechanism induced by elevated temperature in arthropods, experiments were
285 performed in an invertebrate model system (*Drosophila* S2 cells). Literature reports
286 that the temperature range for optimal growth of *Drosophila* S2 cells is 25–28 °C, and
287 S2 cells tolerated a normal growth temperature of 30 °C. Therefore, S2 cells were
288 cultured at normal temperature (27 °C) or high temperature (30 °C) with or without
289 DCV infection. The results showed that S2 cells were adherent to the wall and grew
290 well at 27 °C or 30 °C without DCV infection, and the cytopathic signs of S2 cells were
291 milder at 30 °C than the control group at 27 °C when infected with DCV
292 (Supplementary Fig. 4A). Additionally, the mRNA and protein expression of DCV was
293 significantly lower at 30 °C than the control group at 27 °C (Supplementary Fig. 4B
294 and 4C). These results suggest that elevated temperature could restrict the replication
295 of DCV in *Drosophila* S2 cells.

296 To determine whether DmHSF1 is related to high temperature (30 °C) and DCV
297 infection in S2 cells, its expression level was also determined. The results showed that
298 the mRNA expression of DmHSF1 was significantly upregulated 4.53-fold and 6.48-
299 fold at high temperature (30 °C) or infected with DCV, respectively (Fig. 8A).
300 Antimicrobial peptides have been proven to participate in the innate immunity of

301 *Drosophila* in response to viral infection. The expression of DmAMPs (Attacin A,
302 Cecropins A, Defensin, Metchnikowin, and Drosomycin) was explored in response to
303 high temperature (30 °C) and DCV infection. The results showed that Atta, CecA, and
304 Def were significantly upregulated 5.77-fold, 4.55-fold, and 5.40-fold at high
305 temperature (30 °C), respectively (Fig. 8B). When stimulated by DCV, Atta, CecA, Def,
306 Met, and Drs were remarkably increased 46.84-fold, 123.52-fold, 39.72-fold, 41.14-
307 fold, and 241.40-fold, respectively (Fig. 8C). These results suggest that DmAMPs play
308 a crucial role in anti-DCV defense at high temperature (30 °C).

309 Next, DmHSF1's role in *Drosophila* during DCV infection at high temperature
310 (30 °C) was investigated. Using the RNAi strategy in S2 cells, it was observed that the
311 transcription levels of DmHSF1 can be downregulated by dsRNA-DmHSF1 with or
312 without DCV infection (Fig. 8D). After DmHSF1 knockdown, the mRNA and protein
313 expression of DCV was significantly higher at 30 °C than the control group (Fig. 8E
314 and 8e). Additionally, Atta, CecA, and Def were significantly downregulated 0.65-fold,
315 0.43-fold, and 0.56-fold in DmHSF1 silenced, DCV infected S2 cells at high
316 temperature (30 °C), respectively (Fig. 8F). Furthermore, S2 cells were transfected with
317 pAc5.1a-DmHSF1-HA or pAc5.1a-HA plasmid (as control; Supplementary Fig. 5A).
318 The results showed that the mRNA and protein expression of DCV was significantly
319 lower at 30 °C than the control group (Fig. 8G and 8g). Accordingly, Atta, CecA, and
320 Def were significantly upregulated 4.38-fold, 1.89-fold, and 3.13-fold at high
321 temperature (30 °C), respectively (Fig. 8H). These results show that high temperature
322 (30 °C) and DCV could induce the expression of DmHSF1 and DmAMPs, with
323 DmHSF1 playing crucial roles in defending against DCV at elevated temperatures.

324 To further verify whether DmHSF1 exerts its anti-DCV function by regulating
325 DmAMPs at high temperature (30 °C), the regulatory roles of DmHSF1 on DmAMPs
326 were investigated through ectopic expression of DmHSF1 and knockdown of DmAMPs
327 during infection (Supplementary data). Firstly, the promoter region of DmAtta,
328 DmCecA, and DmDef was cloned, each containing three conserved HSE motifs (Fig.
329 8I). Dual-luciferase reporter assays showed that the promoter of DmAtta, DmCecA,
330 and DmDef could be upregulated 12.36-fold, 7.76-fold, and 2.71-fold by DmHSF1,

respectively. The mutant HSE motifs promoter of DmAtta, DmCecA, and DmDef could not be regulated by DmHSF1 (Fig. 8J). Then, to further demonstrate that DmHSF1 exerts its anti-DCV function by regulating DmAMPs, DmAtta was chosen as a representative. After knockdown of DmAtta (Supplementary Fig. 5B), S2 cells were transfected with DmHSF1 and then infected with DCV. The results showed that the mRNA and protein expression of DCV was significantly lower at 30 °C than the control group (Fig. 8K and 8k). These results suggest that DmHSF1 exerts its anti-DCV function by regulating DmAMPs at high temperature (30 °C).

340 **3. Discussion**

341 Temperature is a key factor regulating various biological activities, and for aquatic
342 ectotherms, it significantly affects growth rates and is also a crucial determinant of viral
343 disease outbreaks (Marcogliese, 2008). Accumulating evidence has indicated that
344 increased temperature enhances immune competence, resistance to infection, and levels
345 of immune mediators under febrile conditions (Evans et al., 2015; Hasday and Singh,
346 2000). High temperatures (32-33 °C) have been shown to inhibit the replication of
347 WSSV and reduce mortality in WSSV-infected shrimp (Sun et al., 2014). Studies have
348 reported that WSSV-infected shrimp reared at high temperatures (above 31 °C) exhibit
349 increased total hemocyte count (THC), phenoloxidase (PO) activity, and apoptotic
350 index (Granja et al., 2003; Wu et al., 2015). However, the mechanism contributing to
351 enhanced pathogen resistance in shrimp at high temperatures remains unclear. In this
352 study, our findings revealed the molecular mechanism through which the HSF-AMPs
353 axis mediates host resistance to viruses induced by febrile temperature. Specifically,
354 AMPs are a newly documented type of effector protein targeted by HSF that mediate
355 the host antiviral response beyond the classical heat shock response.

356 Regulating body temperature, particularly increasing it (fever), is one of the
357 primary defense mechanisms in homeotherms against infections (Hasday et al., 2014).
358 Ectotherms as diverse as reptiles, fish, insects, and crustaceans also raise their core
359 temperature during infection through behavioral regulation, seeking warmer
360 environments—a phenomenon known as behavioral fever (Hasday et al., 2014). This
361 feature, preserved in endothermic mammals and birds, strongly suggests that febrile
362 temperatures confer a survival advantage (Bicego et al., 2007). In 1975, Kluger and
363 colleagues published the first direct experimental study demonstrating the benefits of
364 elevated temperature for infected animals (Kluger et al., 1975). In this study,
365 *dipsosaurus dorsalis*, being poikilothermic animals, were moved from an environment
366 of 36 °C to 40 °C after bacterial infection, resulting in an increase in survival rates from
367 25% to 65% (Kluger et al., 1975). Similar results have since been observed in other
368 poikilotherms and some homeotherms. For instance, carp infected with Cyprinid
369 herpesvirus 3 (CyHV-3) move from lower temperatures of 24-28 °C to 32 °C, where

370 their survival rate reaches 100%, and viral load is significantly reduced (Rakus et al.,
371 2017). Behavioral fever responses to microbial infections have also been reported in
372 aquatic invertebrates such as freshwater crayfish (*Cambarus bartoni*), American lobster
373 (*Homarus americanus*), pink shrimp (*Penaeus duorarum*), horseshoe crab (*Limulus*
374 *polyphemus*), and *Penaeus vannamei* (Casterlin and Reynolds, 1978, 1979; M.E.
375 Casterlin, 1977; Rakhshaninejad et al., 2023). Despite these observations, the
376 antimicrobial immune mechanisms induced by febrile temperatures remain unclear.
377 The prevailing view that febrile temperatures benefit the host primarily suggests that
378 febrile response enhances innate and adaptive immune mechanisms in homeotherms
379 (Hasday et al., 2014). Our findings in the present study further support the enhancement
380 of innate immune mechanisms by febrile temperature in ectotherms such as shrimp and
381 *Drosophila*. Additionally, elevated temperatures can cause some pathogenic
382 microorganisms to lose their optimal growth conditions. However, some
383 microorganisms have evolved strategies to exploit fever to enhance their invasion and
384 proliferation (Freitas Lione et al., 2010; Loh et al., 2013). Paradoxically, this further
385 underscores the benefits of fever for the host, as effective immune strategies exert
386 evolutionary pressure on pathogens, driving them to evolve counterstrategies to hijack
387 or block the febrile response.

388 HSFs are a type of evolutionarily conserved transcription factors initially known
389 for regulating the heat shock response (Anckar and Sistonen, 2011). However,
390 accumulating evidence indicates multiple additional functions beyond the activation of
391 HSPs, including roles in metabolism, immunity, and disease (Barna et al., 2018). HSF1
392 acts through a regulated upstream promoter element called the heat shock element
393 (HSE). HSEs are highly conserved, including the inverted repeats of the pentameric
394 sequence nGAAn (Amin et al., 1988). The type of HSEs found in the proximal promoter
395 regions of HSP genes comprises at least three contiguous inverted repeats consisting of
396 nTTCnnGAAnnTTCn (Xiao and Lis, 1988). The discovery of novel HSF1 target genes
397 not involved in the heat shock response suggests that HSEs may be present in multiple
398 genes beyond HSPs (Barna et al., 2018). For instance, HSF1 can bind to the promoters
399 of CUP1, BTN2, SIS1, SGT2, and SSA3 genes, upregulating their transcriptional

activity to regulate oxidative stress (Morano et al., 2012). HSF1 also regulates the hypothalamic-specific expression of the heat-inducible ion channel gene TRPV1, suggesting a protective effect during fever (Fan-xin et al., 2012). In the present study, we showed that a newly identified antimicrobial peptide, nSWD, is specifically regulated by LvHSF1 via two HSE motifs with the typical nGAAn sequence. Additionally, the promoters of DmAMPs, such as Atta, CecA, and Def, also contain several HSE motifs and are regulated by DmHSF1. Previous studies showed that the upstream sequence of CrustinPm5 contains a putative promoter with an HSE motif, and the expression of CrustinPm5 is upregulated upon heat treatment. However, there is currently no evidence that HSF1 directly binds to the HSE motif of AMPs in invertebrates. Notably, our work is the first to show that HSF1 directly binds to the HSE motifs of AMPs in shrimp and *Drosophila*, suggesting this may be a conserved regulatory mechanism in arthropods.

Although febrile temperature is generally believed to enhance host immunity, the role of heat shock factors (HSFs) in viral infections is complex and varies across different species and types of viral infections (Reyes et al., 2022). In vertebrates, HSF1 has been reported to participate in the transcription of HIV genes and their reactivation from latency (Pan et al., 2016). Additionally, after orthopoxvirus infection, HSF1 is phosphorylated, translocated into the nucleus, and increases the transcription of HSF1 target genes, benefiting the virus by extending the viral genome (Filone et al., 2014). Conversely, stress-independent activation of HSF1 can reduce the quantity and infectivity of HIV copies in a lymphoblastic cell line (Nekongo et al., 2020). Another study reported that HSF1 could enable apoptosis-stimulating protein to reduce autophagy in hepatocytes and inhibit HBV replication (Wang et al., 2021). In invertebrates, DmHSF1-deficient adult flies are hypersensitive to DCV infection, although the underlying mechanism has not yet been uncovered (Merkling et al., 2015). HSF1 is also required for tolerance against several pathogenic agents in *Caenorhabditis elegans* (Singh and Aballay, 2006). Similarly, the present study showed that HSF1 plays a crucial role in antiviral immunity against WSSV infection, with knockdown of HSF1 *in vivo* leading to higher virus copies and increased susceptibility to WSSV infection at

high (32 °C) temperature. Notably, a recent study showed that ammonia stress-induced MjHSF1 upregulates the expression of negative regulators that inhibit the production and function of interferon analogs, enhancing WSSV infection in shrimp *Marsupenaeus japonicus* (Wang et al., 2024). This may be because ammonia stress suppresses host immunity and increases sensitivity to pathogenic infection in aquaculture (Weihrauch et al., 2018). In fact, previous studies have shown that the optimal water temperature for *M. japonicus* growth ranges from 25 to 32 °C, and a high temperature of 31 °C can reduce mortality of WSSV-infected *M. japonicus* without increasing host immune response activity (You et al., 2010). In contrast, the tolerance temperature for *L. vannamei* growth ranges from 7.5 to 42 °C, and our findings showed that elevated temperature can effectively enhance the host's response to WSSV infection (Millard et al., 2021). Evidence also supports the involvement of heat shock proteins in WSSV tolerance at elevated temperatures, with heat shock protein 70 (HSP70) playing a crucial role in inhibiting WSSV replication at high temperatures (32 °C) (Lin et al., 2011; Sun et al., 2014). These findings suggest that the mechanism of elevated temperature protection against WSSV infection differs between *M. japonicus* and *L. vannamei*. Therefore, our findings, together with those of other studies, suggest that the benefit of HSF1 can be attributed to either the host or the pathogen, depending on the nature and context of the host-virus-environment interaction.

Antimicrobial peptides (AMPs) are pivotal components of innate immunity in invertebrates, serving as the first line of defense against invading pathogens, including bacteria, fungi, and viruses (Brogden, 2005). Typically, the transcription of AMPs is regulated by the classical NF-κB and JAK/STAT pathways in invertebrates (Carpenter and O'Neill, 2024). However, our results revealed that AMPs can also be regulated by an alternative pathway mediated by HSF1 in shrimp and *Drosophila*. In crustaceans, various AMP families, including penaeidins, anti-lipopolysaccharide factors, crustins, and stylicins, have been identified (Matos and Rosa, 2022). Among these, the newly identified nSWD belongs to type III crustins, characterized by a single WAP domain (SWD) and a short N-terminal region. The most probable anti-WSSV mechanism of nSWD is its direct interaction with WSSV envelope proteins VP24 and VP26,

460 potentially inhibiting viral entry into target cells. VP24 has been identified as a WSSV
461 receptor-binding protein, interacting with the cellular receptor pIgR to mediate WSSV
462 entry into host cells (Niu et al., 2019). VP26 has been reported to bind to SNAP29,
463 inhibiting SNARE complex assembly and autophagic degradation (Liu et al., 2024).
464 Additionally, WSSV VP24, VP26, and VP28 form a complex termed an "infectosome",
465 which is crucial for WSSV infectivity (Li et al., 2015). Therefore, the binding of nSWD
466 to WSSV envelope proteins VP24 and VP26 could disrupt WSSV integrity and
467 attenuate viral entry into shrimp cells.

468 In conclusion, our study demonstrates a conserved antiviral febrile response,
469 where the elevated temperature-induced HSF1-AMP axis plays a crucial role in
470 enhancing host resistance to viruses in shrimp and *Drosophila* (Fig. 9). Specifically,
471 febrile temperature-induced HSF1 induces the expression of AMPs, which directly bind
472 to WSSV envelope proteins and inhibit WSSV proliferation. Additionally, high
473 temperature restricts DCV replication in the invertebrate model system *Drosophila*,
474 also mediated by the HSF1-AMPs cascade. These findings highlight previously
475 unforeseen roles of HSF1 beyond the traditional heat shock response, revealing its
476 involvement in thermal regulation of immunity and the innate immune system's
477 response to thermal stress. Moreover, this study provides new avenues for managing
478 viral infections in arthropods, suggesting that environmental control can effectively
479 enhance disease resistance.

480

481

482 **4. Materials and methods**

483 ***Animal and pathogens***

484 Healthy specimens of *L. vannamei*, averaging 5 g each, were utilized for our
485 experiments. These specific pathogen-free (SPF) shrimp were sourced from Hisenor
486 Company's shrimp farm in Maoming, Guangdong Province, China. The shrimp were
487 maintained in a recirculating water tank system filled with air-pumped seawater at a
488 salinity of 25‰ and a constant temperature of 25 ℃. They were fed thrice daily to
489 satiation with a commercial shrimp diet provided by HAID Group, Guangzhou, China.
490 The inoculum for the WSSV, Chinese strain (AF332093), was prepared following
491 previously described methodologies (Li et al., 2018).

492 WSSV was extracted from the muscle tissue of WSSV-infected shrimp and
493 subsequently stored at –80 ℃. Prior to injection, the muscle tissue was homogenized
494 to prepare the WSSV inoculum, containing approximately 1 × 10^5 copies in 50 μl of
495 Phosphate-Buffered Saline (PBS; 140 mM NaCl, 2.7 mM KCl, 10 mM Na_2HPO_4, 1.8
496 mM KH_2PO_4, pH 7.4). For the pathogenic challenge experiments, each shrimp was
497 administered an intraperitoneal injection of 50 μl of the WSSV solution into the second
498 abdominal segment. Injections were performed using a 1-ml syringe (Becton Dickinson,
499 Shanghai, China).

500 Drosophila C Virus (DCV) were kindly provided by Professor Jiahuai Han's Lab.
501 The DCV was amplified in the S2 cells, after 3 days of infection, culture medium was
502 collected and centrifuged at 4 ℃ for 20 min (2,000 × *g*), then the supernatant was
503 collected and aliquots were frozen at –80 ℃.

504

505 ***Cells and cells assays***

506 *Drosophila* S2 cells (ATCC CRL 1963) were cultured at 28 °C in Schneider's Insect
507 Medium (Sigma-Aldrich, St. Louis, MO, USA) containing 10% fetal bovine serum
508 (Gibco, Grand Island, NY).

509 To knockdown *DmHSF1 in vitro*, 8 ×10^6 S2 were transfected with 15 μg dsRNA
510 in a 6-well plate by using FuGENE® HD Transfection Reagent (Promega Shanghai,
511 China), and transfected cells were incubated at 27 ℃ for 3 days before the transfection

512 and DCV infection assays according to a previously published method (Yang et al.,
513 2018).
514 For temperature assays, S2 cells were seeded into 6-well plate and then incubated
515 at 27 ℃ or 30 ℃ for 24 h, the transcription of DCV and DmHSF1 were detected by
516 qPCR. Besides, the same numbers of dsRNA-treated cells were infected with DCV at
517 a multiplicity of infection (MOI) of 10 in a 6-well plate at 27 ℃ or 30 ℃ for 24 h and
518 replaced with fresh medium, and the total RNA of S2 cells were extracted for qPCR
519 analysis.
520
521 ***Transcriptomic analysis***
522 Two groups of *L. vannamei* shrimp, Group W and Group TW, each comprising 30
523 individuals, were initially cultured at 25 ℃. For Group W, the shrimp were injected
524 with WSSV and continuously maintained at 25 ℃. In contrast, Group TW shrimp were
525 also injected with WSSV, but the culture temperature was raised to 32 ℃ within 3 hours
526 at 24 hours post-injection (hpi). At 12 hours post-temperature raising (hptr), gill
527 samples from 8 shrimp in both Group W and Group TW were collected. These samples
528 were immediately preserved in liquid nitrogen for subsequent analysis. Transcriptomic
529 sequencing was performed by LianChuan Biotech (Hangzhou, China). The FPKM
530 value was used to represent gene expression levels in each sample. The differential
531 expression between the two groups, each with three biological replicates, was
532 determined using DESeq2 software, accepting criteria of log2 (Fold Change) ≥ 1 and
533 an adjusted p-value ≤ 0.05. Gene annotations were provided for the *L. vannamei* shrimp
534 genome (Zhang et al., 2019). OmicShare tools (www.omicshare.com/tools) was used
535 to predict potential transcription factors and generate a heatmap.
536 To identify the genes whose expression was regulated by *LvHSF1*, healthy shrimp
537 were administered an intramuscular injection of 10 μg dsRNA targeting the *LvHSF1*
538 gene or *GFP* as a control. After 48 hours, shrimp were injected with 1×10^5 copies of
539 WSSV. At 24 hours post WSSV challenge, gill samples from 8 shrimp in both *dsHSF1*
540 and *dsGFP* were collected. These samples were immediately preserved in liquid
541 nitrogen for subsequent analysis. The sequencing and heatmap were performed

542 similarly to the above procedure.

543

544 ***RNA extraction, cDNA synthesis, and DNA and protein extraction***

545 Total RNA was extracted from different tissues of shrimp using the Eastep Super
546 Total RNA Extraction Kit (Promega, Shanghai, China). The genomic DNA of shrimp
547 tissues was extracted using a genomic DNA extraction kit (Vazyme, Nanjing, China).
548 First-strand cDNA synthesis was performed using a cDNA synthesis kit (Accurate
549 Biology, Hunan, China), according to the manufacturer's instructions. Protein samples
550 from gills and hemocytes were homogenized separately in IP lysis buffer (25 mM Tris-
551 HCl pH 7.4, 150 mM NaCl, 1 mM EDTA, 1% NP-40, 5% glycerin; Thermo Scientific,
552 Shanghai, China) with a protease and phosphatase inhibitor cocktail (Merck,
553 Kenilworth, NJ, USA), and then centrifuged at 12,000 × *g* for 10 minutes at 4 °C to
554 collect the supernatant for further analysis.

555

556 ***Tissue expression and immune challenge analysis by quantitative real-time PCR***
557 ***(qPCR)***

558 QPCR assays were performed to assess the mRNA levels in tissues expression
559 distribution, immune stimulation or the *in vivo* RNAi experiments. Expression levels
560 of *HSF1* (GenBank accession No. AHI13794), *nSWD* (GenBank accession No.
561 PP786678) and *VP28* (GenBank accession No. NP_477943.1) were detected using
562 LightCycler480 System (Roche, Basel, Germany) in a final reaction volume of 10 μl,
563 which was comprised of 1 μl of 1: 10 cDNA diluted with ddH_2O, 5 μl of SYBR Green
564 Pro Taq HS Mix (Accurate Biology, Hunan, China) and 250 nM of specific primers
565 (Supplementary table 1).

566 For tissue distribution, shrimp were cultured at low temperature (25 °C) and high
567 temperature (32 °C). Shrimp tissues of epithelium, hemocyte, stomach, nerves, eyestalk,
568 gill, antenna, hepatopancreases, muscle, heart, intestine and pleopod were sampled and
569 pooled from 15 shrimp. For immune stimulation, the treated group were injected with
570 5 μg polyinosinic-polycytidylic acid (Poly (I: C)) or 50 μl WSSV (~1×10^5 copies), and
571 the control group was injected with PBS solution. Hemocyte, gill and intestine of

572 challenged shrimps were collected at 0, 4, 8, 12, 24, 36, 48, and 72 h after injection.
573 The cycling program were performed as described previously (Xiao et al., 2021). The
574 expression of each gene was calculated using the Livak ($2^{-\Delta\Delta CT}$) method after
575 normalization to *EF-1α* (GenBank accession No. GU136229) and *β-Actin* (GenBank
576 accession No. AF186250). Primer sequences are listed in Supplementary table 1.
577 The transcription of *DCV*, *DmHSF1* (GenBank accession No. NM_057227.5) and
578 *DmAMPs* were also detect by quantitative real-time PCR. The expression of each gene
579 was calculated using the Livak ($2^{-\Delta\Delta CT}$) method after normalization to *DmRpL32*
580 (GenBank accession No. NP_733340.1). Primer sequences are listed in Supplementary
581 table 1.
582
583 ***Detection of viral loads by absolute quantitative PCR***
584 To measure viral titers in shrimp, absolute quantitative PCR (ab-qPCR) was
585 employed. This process utilized a set of primers, wsv069 (WSSV32678-
586 F/WSSV32753-R), targeting a single-copy gene of the WSSV, along with a Taq-Man
587 fluorogenic probe (WSSV32706), as detailed in previous studies. Gill tissue samples
588 were collected from WSSV-infected shrimp. DNA extraction from these samples was
589 conducted using previously described methods (Fu et al., 2022). The concentration of
590 WSSV genome copies was quantified by ab-qPCR, using the specific primers
591 WSSV32678-F/WSSV32753-R and the TaqMan fluorogenic probe, as listed in
592 Supplementary table 1. To ensure accuracy, each shrimp sample underwent three
593 replicates of ab-qPCR. The number of WSSV genome copies was calculated and
594 normalized against 0.1 μg of shrimp tissue DNA.
595
596 ***Recombinant protein expression and purification***
597 The coding sequences of nSWD (without the signal peptide, 1-26 amino acids) was
598 amplified by PCR using corresponding primers (Supplementary table 1) and subcloned
599 into pET-32a (+) plasmid (Merck Millipore, Darmstadt, Germany). After confirmed by
600 sequencing, the recombinant plasmid was transferred into *E. coli* Rosetta (DE3) cells
601 (TransGen Biotech, Beijing, China). Then, positive clones harboring the desired

602 fragment were selected for inducing expression. After 4 hours of induction with 0.1
603 mM Isopropyl β-D-Thiogalactoside (IPTG) at 30 ℃, cells were pelleted by
604 centrifugation and sonicated for 30 minutes on ice water. The supernatant from the
605 sonicated proteins was purified by using Ni-NTA agarose (Qiagen, Düsseldorf,
606 Germany) according to the manufacturer's instructions. The rTrx-His-tag, GST and
607 HSF1-GST proteins were induced and purified in the same way. The purified proteins
608 were checked by Coomassie staining or Western blot analysis. The concentration of the
609 purified proteins was determined using a BCA protein assay kit (Beyotime
610 Biotechnology, Shanghai, China).
611
612 ***SDS-PAGE and western blotting***
613 Western blotting was performed to evaluate the protein levels of LvHSF1, VP28,
614 DCV, the purified nSWD, rTrx-His-tag and LvHSF1-GST. And then the proteins were
615 separated on 12.5% SDS-PAGE gels and then transferred to polyvinylidene difluoride
616 (PVDF) membranes (Merck Millipore, Darmstadt, Germany). After blocking with 5%
617 nonfat milk diluted in Tris Buffered Saline with Tween 20 (TBST) buffer (150 mM
618 NaCl, 0.1% Tween-20, 50 mM Tris-HCl, pH 8.0) for 1 hour, and the membrane was
619 incubated with 1: 1000 polyclonal rabbit anti-LvHSF1 (produced in Gene Create,
620 Wuhan, China), 1: 1000 polyclonal rabbit anti-VP28 (produced in Abmart, Shanghai,
621 China), 1: 1000 polyclonal rabbit anti-DCV capsid polyprotein (Abcam, Cambridge,
622 UK), 1:1000 mouse anti-6 × His (Sigma, St Louis, MO, USA) or 1:1000 mouse anti-
623 GST (TransGen Biotech, Beijing, China) for 2 hours at 25 °C. The PVDF membranes
624 were washed for three times with TBST and then incubated with 1:5000 goat anti-rabbit
625 IgG (H+ L) HRP or 1:5000 goat anti-mouse IgG (H+ L) HRP secondary antibody
626 (Promega, Shanghai, China) for 1 hour. Membranes were developed using an enhanced
627 chemiluminescent blotting substrate (Thermo Fisher Scientific, Waltham, MA, USA),
628 and the chemiluminescent signal was detected using the 5200 Chemiluminescence
629 Imaging System (Thermo Fisher Scientific, Waltham, MA, USA).
630
631 ***Knockdown of specific genes by RNA interference (RNAi)***

632 The T7 RiboMAX Express RNAi System kit (Promega, Shanghai, China) was
633 employed for the synthesis of double-stranded RNA (dsRNA) targeting *HSF1*, *nSWD*
634 and *GFP*. The specific primers used for dsRNA synthesis are listed in Supplementary
635 table 1. The integrity and quality of the synthesized dsRNA were verified using 1.5%
636 agarose gel electrophoresis and quantified with a NanoDrop 2000 spectrophotometer
637 (Thermo Scientific, Shanghai, China). For the experimental treatments, shrimp were
638 injected with 2 μg/g of body weight of the respective dsRNAs, dissolved in 50 μl of
639 PBS. Control groups received injections of GFP dsRNA and PBS. Hemocytes and gills
640 were collected from the shrimp 48 hours post-dsRNA injection. Total RNA was
641 extracted from the collected tissue samples. The efficiency of RNAi was evaluated by
642 qPCR using the corresponding primers for each gene. This assessment aimed to confirm
643 the knockdown of the targeted genes in the experimental groups compared to the
644 controls as described previously (Li et al., 2024).
645
646 ***Survival assays***
647 Healthy shrimp were divided into two groups (n = 30 each) and received an
648 intramuscular injection of 10 μg dsRNA solution (HSF1 dsRNA or GFP dsRNA diluted
649 in PBS). After 48 hours post dsRNA injection, the shrimp in each group were injected
650 again with 1×10^5 copies of WSSV particles diluted in 50 μl PBS. The first group was
651 maintained at low temperature (25 °C), the second at a high temperature (32 °C). The
652 survival rates of each group were recorded at 4-hour intervals.
653 To knockdown the expression of nSWD, healthy shrimp were administered an
654 intramuscular injection of 10 μg dsRNA targeting the *nSWD* gene or PBS as a control.
655 After 48 hours, shrimp were injected with 1×10^5 copies of WSSV, with a parallel group
656 receiving a mock challenge with PBS (n = 30). To evaluate the effect of recombinant
657 rnSWD on WSSV replication *in vivo*, rescue experiments were conducted. Shrimp (n =
658 30) were co-injected with 10 μg rnSWD or rTRX along with the WSSV inoculum. The
659 survival rates of each group were recorded at 4-hour intervals. Differences in survival
660 between groups were analyzed using the Mantel-Cox (log-rank χ^2 test) method,
661 employing GraphPad Prism software (GraphPad Software, La Jolla, CA, USA).

662

663 ***Dual-luciferase reporter assays***

664 The partial promoter sequence with 2000 bp upstream of nSWD was cloned using
665 the specific primers (Supplementary table 1) and then linked into pGL3-Basic (Promega,
666 Shanghai, China) to generate pGL3-nSWD (reporter plasmid). The vector pGL3-
667 nSWD-M1, pGL3-nSWD-M2 and pGL3-nSWD-M12 with mutant of the HSF1 binding
668 motif were also generated, respectively. *Drosophila* S2 cell was used instead in order
669 to detect the effects of HSF1 on the promoters of nSWD. For dual-luciferase reporter
670 assays, S2 cells were plated into a 96-well plate, and 12 hours later, the cells of each
671 well were transfected with 0.05 μg of firefly luciferase reporter gene plasmids, 0.001
672 μg pRL-TK renilla luciferase plasmid (Promega Shanghai, China), or 0.05 μg proteins
673 expression plasmids or empty pAc5.1A plasmids (as controls) using the Fugene HD
674 Transfection Reagent (Promega Shanghai, China) according to the user manual. Forty-
675 eight hours post-transfection, the dual-luciferase reporter assays were performed in
676 order to calculate the relative ratios of firefly and renilla luciferase activities using the
677 Dual-Glo Luciferase Assay System kit (Promega Shanghai, China), according to the
678 manufacturer's instructions. All experiments were repeated six times.

679 To explore the regulatory activity of DmHSF1 on the DmAMPs (Atta, CecA and
680 Def), we constructed the vector pGL3-Atta, pGL3-CecA and pGL3-Def. And the vector
681 pGL3-Atta, pGL3-CecA and pGL3- Def with mutant of the HSF1 binding motif were
682 also generated, respectively. The dual-luciferase reporter assays were conducted in the
683 same way.

684

685 ***EMSA assay***

686 EMSA was performed using a Light Shift Chemiluminescent EMSA kit (Thermo
687 Fisher Scientific, Waltham, MA, USA) according to a previously published method
688 (Wang et al., 2020). Briefly, the biotin-labeled or unbiotin-labeled probes were designed
689 using the *HSF1* binding motif sequence (5'- CTATAGAACCATC-3' and 5'-
690 GACTTTTCGAGGA -3'). The mutant probe was designed via mutating the HSF1
691 binding motif sequence. All of the probes were synthesized by Ruibo Technologies

692 (Guangzhou, China), and sequences are listed in Supplementary table 1. In brief, the
693 recombinant proteins (10 μg) of HSF1 were incubated with 20 fmol of the probes for
694 the binding reactions. The reactions were separated on a 5% native PAGE gel,
695 transferred to positively charged nylon membranes (Roche, Germany), and cross-linked
696 by UV light. Then the biotin-labeled DNA on the membrane was detected by
697 chemiluminescence and developed on x-ray film, followed by enhanced
698 chemiluminescence (ECL) visualization (Tanon, Shanghai, China).
699
700 ***Pull-down assays***
701 Pull-down assays were performed to explore whether the recombinant rnSWD
702 could interact with the main envelope proteins of WSSV (VP19, VP24, VP26 and
703 VP28). The recombinant GST-tagged VP19, VP24, VP26 and VP28 were obtained from
704 our previous studies (Xiao et al., 2020). For GST pull-down assays, 5 μg rnSWD was
705 incubated with 5 μg of GST-tagged WSSV protein solution at 4 °C for 3 h by agitation.
706 Subsequently, 20 μl of the GST resin were added and the agitation continued for another
707 2 h. The resin was washed four times with PBS. Finally, the resins were re-suspended
708 in 50 μl of the SDS-PAGE sample buffer, boiled and analyzed by Western blot analysis
709 using 6 × His antibody. For His pull-down assays, 5 μg rnSWD was incubated with 5
710 μg of GST-tagged WSSV protein solution at 4 °C for 3 h by agitation. Subsequently, 20
711 μl of the Ni-NTA binding resin were added and the agitation continued for another 2 h.
712 The resin was washed four times with PBS. Finally, the resins were re-suspended in 50
713 μl of the SDS-PAGE sample buffer, boiled and analyzed by Western blot analysis using
714 GST-tag antibody.
715
716 ***Immunocytochemical staining***
717 Immunocytochemical staining was used to observe the co-localization of nSWD
718 and WSSV VP proteins. *Drosophila* S2 cells were seeded onto poly-L-lysine-treated
719 glass cover slips in a 24-well plate with approximate 40% confluent. The S2 cells of
720 each well were transfected with 0.5 μg pAc5.1-nSWD-Flag, pAc5.1-VP24-HA or
721 pAc5.1-VP26-HA using the MIK-3000 Transfection Reagent (MIKX, Shenzhen,

722 China). Thirty-six hours post plasmid transfection, cell culture medium was removed,
723 and cells washed with PBS three times. Cells were then fixed with 4%
724 paraformaldehyde at 25 °C for 15 min following with methanol permeabilization at -
725 20 °C for 10 min. After washing sides for three times, cells were blocked with 3%
726 bovine serum albumin (dissolved in PBS) for 60 min at 25 °C and then incubated with
727 rabbit anti-HA antibody (CST, 1:300 diluted in 2% BSA) and mouse anti-Flag antibody
728 (CST, 1:300 diluted in 2% BSA). The slides were then washed with PBS three times
729 and then incubated with anti-rabbit IgG (H+L) Alexa Fluor 488 (CST, 1:1000 diluted
730 in 2% BSA) and anti-mouse IgG (H+L) Alexa Fluor 594 (CST, 1:1000 diluted in 2%
731 BSA) for 60 min at 25 °C in the dark. The cell nuclei were stained with Hoechst
732 (Beyotime, Shanghai, China; cat. no. C1002) for 5 min. Finally, fluorescence was
733 visualized on a confocal laser scanning microscope (Leica TCS-SP8, Wetzlar,
734 Germany).
735
736 ***Statistical analysis***
737 All data were presented as means ± SD. Student's *t* test was used to calculate the
738 comparisons between groups of numerical data. For survival rates, data were subjected
739 to statistical analysis using GraphPad Prism software (Graphpad, San Diego, CA, USA)
740 to generate the Kaplan–Meier plot (log-rank χ^2 test).
741
742
743
744
745
746
747
748
749
750
751

Declaration of interest statement: All authors declare that the research was conducted in the absence of any commercial or financial relationships that could be construed as a potential conflict of interest.

Author contributions: Chaozheng Li, Jianguo He and Bang Xiao conceived and designed the experiments. Bang Xiao, Shihan Chen, Yue Wang, Xuzheng Liao and Chaozheng Li performed the experiments and analyzed data. Bang Xiao, Shihan Chen, Yue Wang, Xuzheng Liao and Chaozheng Li wrote the draft manuscript. Chaozheng Li and Jianguo He acquired finding. Chaozheng Li was responsible for forming the hypothesis, project development, data coordination, and writing, finalizing, and submitting the manuscript. All authors discussed the results and approved the final version.

Acknowledgement: This research was supported by Southern Marine Science and Engineering Guangdong Laboratory (Zhuhai) (SML2023SP234), National Natural Science Foundation of China (32022085/31930113/32373158), China Postdoctoral Science Foundation (2023M743987), and Guangdong Basic and Applied Basic Research Foundation (2023A1515110528). The funders had no role in study design, data collection and analysis, decision to publish, or preparation of the manuscript.

Data availability: All reagents and experimental data are available within transparent methods or from corresponding author upon reasonable request.

Ethics statement: All animal experiments were approved by Institutional Animal Care and Use Committee of Sun Yat-Sen University (Approval No. SYSU-IACUC-2023-B0005).

781 **Figures and Figure legends**

782 **Figure 1.**

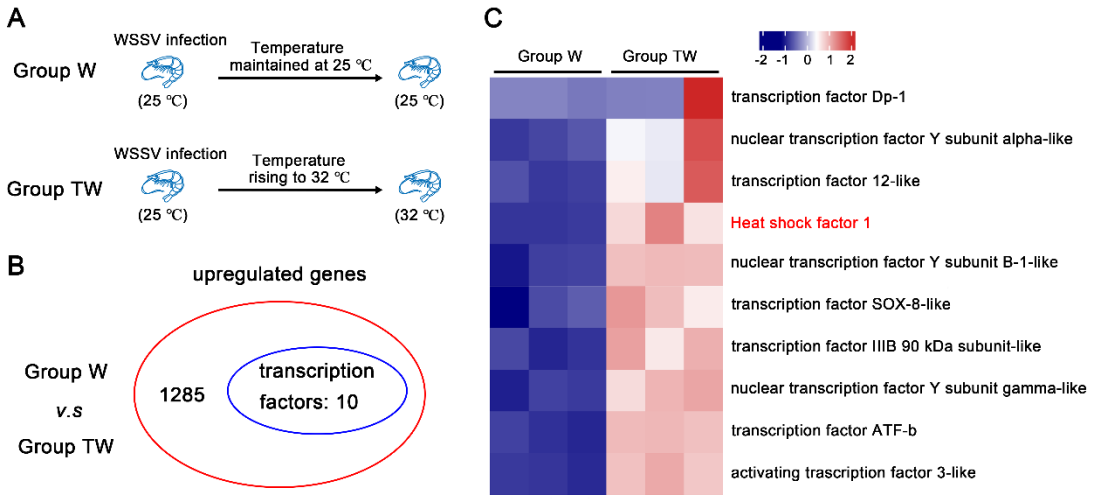

783

784 **Figure 1. Identification of HSF1 as a key factor induced by high temperature.**

785 **(A)** Diagram illustration of the experimental setup for transcriptome analysis. Group W
786 was injected with WSSV and maintained continuously at 25 °C. In contrast, Group TW,
787 also injected with WSSV, had their culture temperature increased to 32°C at 24 hours
788 post-injection (hpi).

789 **(B)** Identification of high temperature-induced genes by RNA-Seq. RNA sequencing
790 was performed 12 hours post-temperature increase. Gill samples from 8 shrimp in each
791 group were collected for Illumina sequencing (NCBI SRA database accession number
792 PRJNA1050424).

793 **(C)** Heatmap showing the differential expression of upregulated genes encoding
794 potential transcription factors. The heatmap displays the fragments per kilobase per
795 transcript per million mapped reads (FPKM) values from three biological replicates,
796 shown after logarithmic transformation.

797

798

799

800 **Figure 2.**

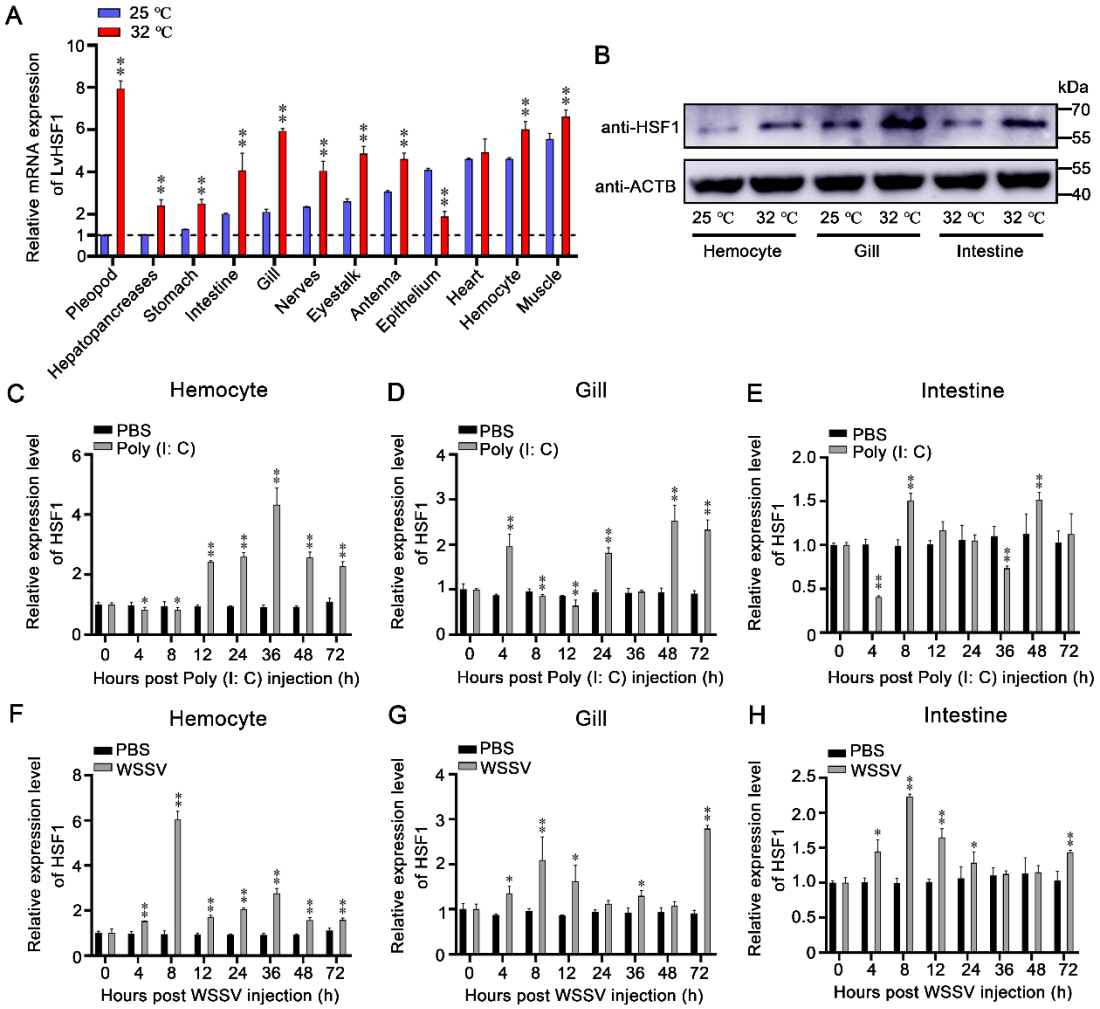

801

802 **Figure 2. Upregulation of LvHSF1 in shrimp challenged by WSSV at both low**
803 **(25 °C) and high (32 °C) temperatures.**

804 **(A)** Transcriptional expression of LvHSF1 in different tissues of healthy shrimp
805 subjected to low (25 °C) and high (32 °C) temperatures. The pleopod tissue at 25 °C
806 serves as a reference, with its expression level set to 1.0. Expression values were
807 normalized against EF-1α and β-Actin using the Livak ($2^{-\Delta\Delta CT}$) method. Data represent
808 the mean ± SD from triplicate assays.

809 **(B)** Protein levels of HSF1 at 25 °C and 32 °C detected by western blotting.

810 **(C-E)** Expression profiles of LvHSF1 after Poly (I:C) injection in hemocytes (C), gills
811 **(D)** and intestines (E). Expression levels were measured by qPCR, normalized against
812 EF-1α and β-Actin using the Livak ($2^{-\Delta\Delta CT}$) method, and presented as mean ± SD from
813 triplicate assays.

(F-H) Expression profiles of LvHSF1 after WSSV injection in hemocytes (F), gills (G) and intestines (H). Expression levels were measured by qPCR, normalized against EF-1α and β-Actin using the Livak ($2^{-\Delta\Delta CT}$) method, and presented as mean ± SD from triplicate assays.

Statistical significance was calculated using the Student's *t*-test (**$p < 0.01$, *$p < 0.05$). All experiments were representative of three biological replicates and yielded similar results.

822 **Figure 3.**

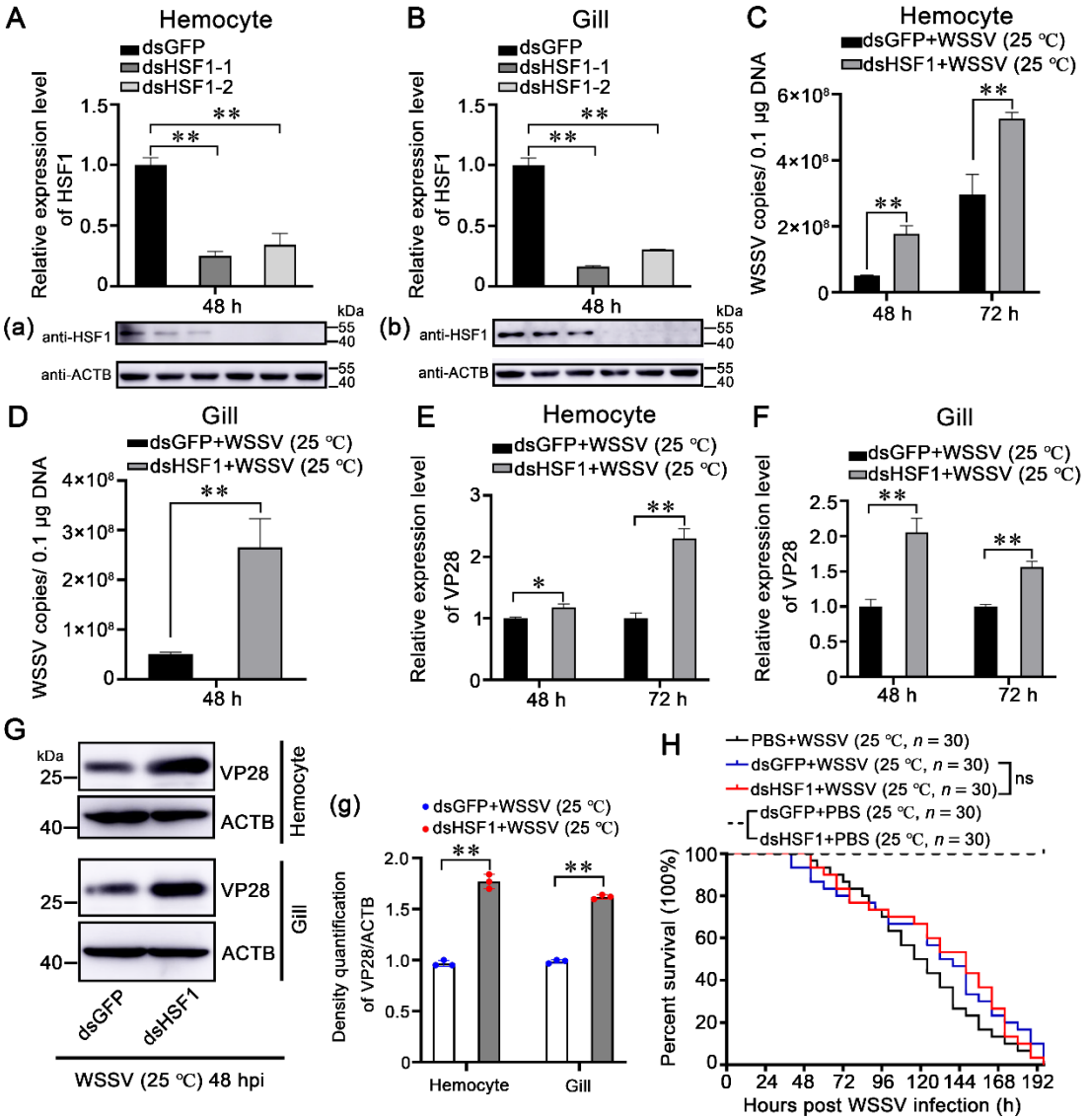

823

824 **Figure 3. Role of HSF1 in restricting WSSV replication in shrimp at low (25 °C)**
825 **temperatures.**

826 **(A, B)** Silencing Efficiency of dsRNA-LvHSF1. The efficacy of two dsRNA-LvHSF1
827 constructs (dsLvHSF1-1 and dsLvHSF1-2) was assessed by qPCR in hemocytes (A)
828 and gills (B). Additionally, protein levels of LvHSF1 were evaluated by western
829 blotting in both tissues (panels a and b). Expression values were normalized against EF-
830 1α and β-Actin using the Livak ($2^{-\Delta\Delta CT}$) method. Data represent the mean ± SD from
831 triplicate assays.

832 **(C, D)** Quantification of WSSV copies. The quantity of WSSV copies in hemocytes (C)
833 and gills (D) at low temperature (25 °C) post-WSSV infection was determined using

absolute quantitative PCR.

(E, F) Transcriptional expression of the VP28 gene. The transcriptional expression of the VP28 gene was analyzed by qPCR in hemocytes (E) and gills (F) at low temperature (25 °C) following WSSV infection.

(G) Expression of WSSV VP28 protein. Expression of WSSV VP28 protein was detected by western blotting in hemocytes and gills at low temperature (25 °C) after WSSV infection. Quantification and statistical analysis of three independent repeats were performed using ImageJ (panel g).

(H) Survival rates of WSSV-infected shrimp post-LvHSF1 knockdown. The survival rates of WSSV-infected shrimp post-LvHSF1 knockdown were monitored at low temperature (25 °C), with recordings made every 4 hours.

Statistical analysis was performed using the Kaplan-Meier plot (log-rank χ^2 test). All experiments were conducted with three biological replicates, consistently yielding similar results.

849 **Figure 4.**

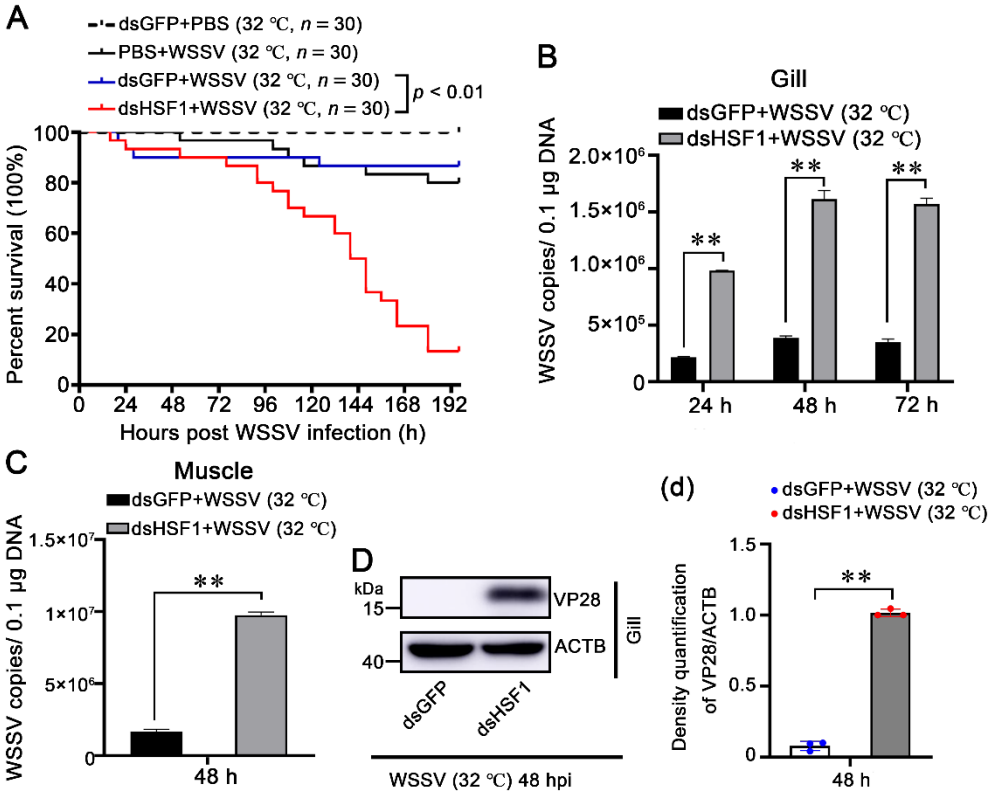

850

851 **Figure 4. Role of HSF1 in restricting WSSV replication in shrimp at high (32 ℃)**
852 **temperatures.**

853 **(A)** Survival rates of WSSV-infected shrimp post-LvHSF1 knockdown. The survival
854 rates of WSSV-infected shrimp post-LvHSF1 knockdown were monitored at high
855 temperature (32 °C), with recordings made every 4 hours. Statistical analysis was
856 performed using the Kaplan-Meier plot (log-rank χ^2 test).

857 **(B, C)** Quantification of WSSV copies. The quantity of WSSV copies in gills (B) and
858 muscles (C) at high temperature (32 °C) post-WSSV infection was determined using
859 absolute quantitative PCR.

860 **(D)** Expression of WSSV VP28 protein. Expression of WSSV VP28 protein was
861 detected by western blotting in gills at high temperature (32 °C) after WSSV infection.
862 Quantification and statistical analysis of three independent repeats were performed
863 using ImageJ (panel d). Statistical significance was calculated using the Student's *t*-test
864 (**$p < 0.01$). All experiments were conducted with three biological replicates,
865 consistently yielding similar results.

866 **Figure 5.**

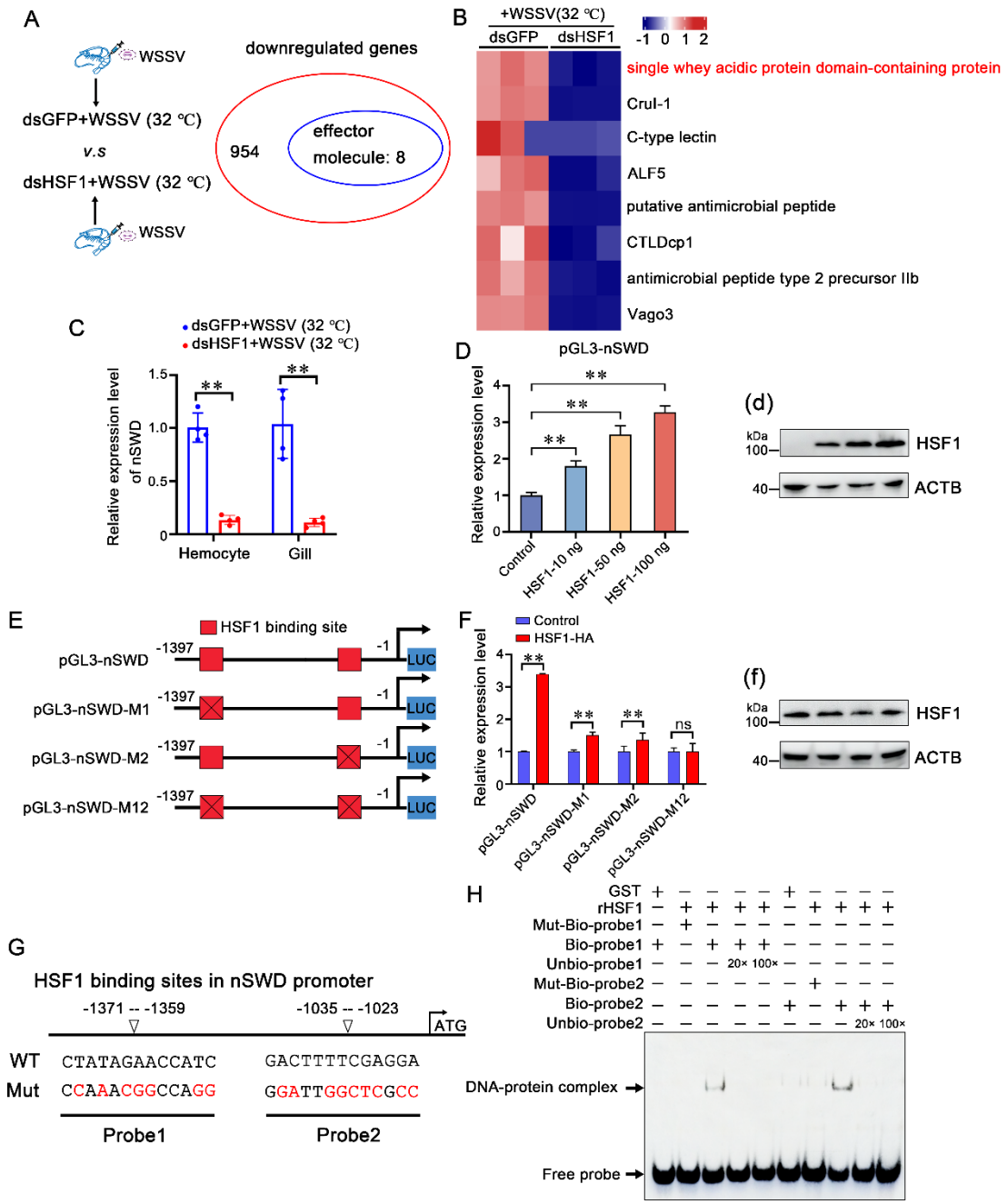

867

868 **Figure 5. nSWD is a potential antiviral effector regulated by HSF1.**

869 **(A)** Venn diagram showing the downregulated genes by RNA-Seq. RNA-seq was
870 performed 24 hours after WSSV infection (NCBI SRA database accession number
871 PRJNA1110613).

872 **(B)** Heatmap showing the differential expression of downregulated genes encoding
873 potential effector molecules. The color bar indicates the gradient of normalized
874 expression levels.

875 **(C)** mRNA transcription levels of nSWD in hemocytes and gills. mRNA transcription
876 levels of nSWD in the hemocytes and gills of LvHSF1-silenced shrimp under WSSV
877 challenge.
878 **(D)** Dual-luciferase reporter assays. Dual-luciferase reporter assays were performed to
879 analyze the effects of overexpression of LvHSF1 on the promoter activities of nSWD
880 in *Drosophila* S2 cells in a dose-dependent manner. Protein expression of LvHSF1 was
881 detected with anti-HA Ab, with β-actin used as a protein loading control (panel d).
882 **(E)** Schematic diagram of the nSWD promoter regions. Schematic diagram of the
883 nSWD promoter regions in the luciferase reporter gene constructs. The HSF1 binding
884 motif sites are shown in red rectangles.
885 **(F)** Dual-luciferase reporter assays with mutated HSF1 binding motifs. Dual-luciferase
886 reporter assays were performed to analyze the effects of overexpression of LvHSF1 on
887 the promoter activities of nSWD with mutated HSF1 binding motifs. Protein expression
888 of LvHSF1 was detected with anti-HA Ab, with β-actin used as a protein loading control
889 (panel f).
890 **(G)** Analysis of the nSWD promoter. The HSF1 binding site was analyzed using the
891 online JASPAR database.
892 **(H)** EMSA assay. LvHSF1 protein interaction with HSF1 binding sites from the nSWD
893 promoter was analyzed *in vitro* by EMSA assay. Competition assays were performed in
894 the presence of excess unlabeled probes.
895 Statistical significance was calculated using the Student's *t*-test (**$p < 0.01$, *$p < 0.05$).
896 All experiments were conducted with three biological replicates, consistently yielding
897 similar results.
898
899
900
901
902
903
904

905 **Figure 6.**

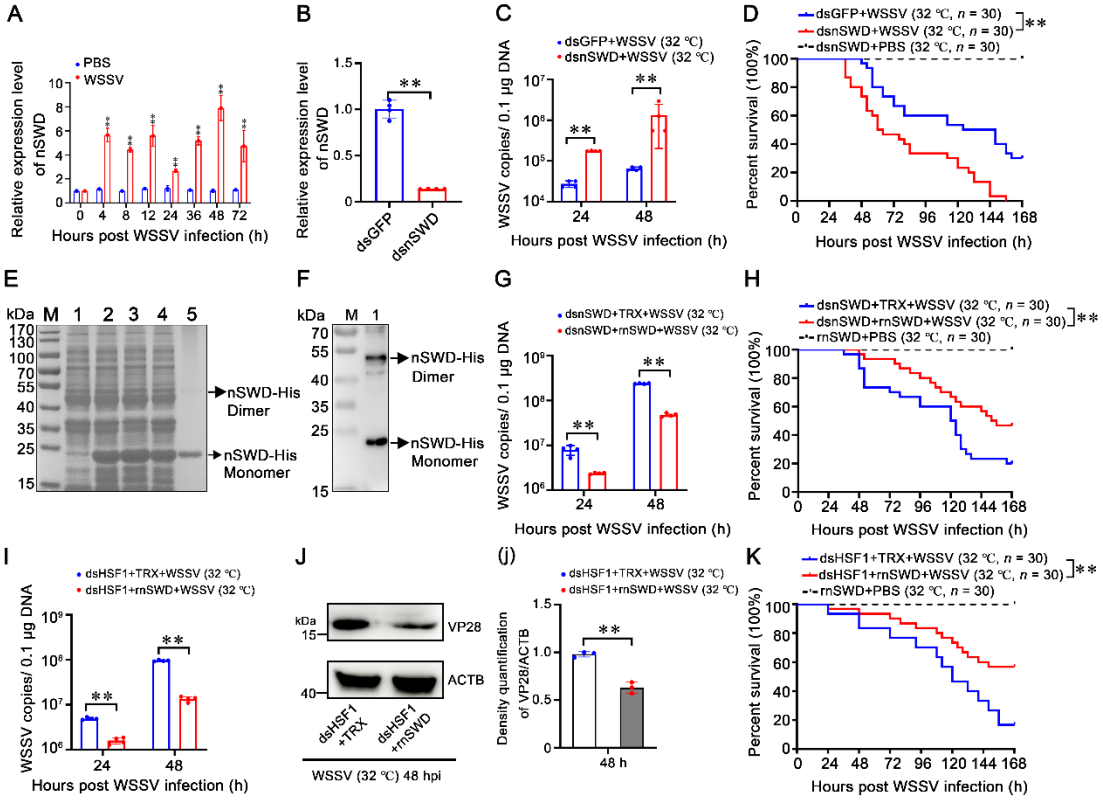

906

907 **Figure 6. *nSWD* possessed potent antiviral activities against WSSV.**

908 **(A)** Expression of nSWD in gills from WSSV-challenged shrimp.

909 **(B)** Silencing efficiency of nSWD in gills. Silencing efficiency of nSWD in gills 48
910 hours after WSSV infection.

911 **(C)** Quantity of WSSV copies in gills at high temperature (32 °C). The quantity of
912 WSSV copies in gills at high temperature (32 °C) was detected by absolute quantitative
913 PCR at 24 and 48 hours after WSSV infection. DsGFP was used as a control.

914 **(D)** Survival rates of WSSV-infected shrimp post-nSWD knockdown. Survival rates of
915 WSSV-infected shrimp post-nSWD knockdown at high temperature (32 °C) were
916 monitored, with recordings made every 4 hours. Statistical analysis was performed
917 using the Kaplan-Meier plot (log-rank χ^2 test).

918 **(E)** SDS-PAGE analysis of recombinant nSWD protein expressed in *E. coli*. Line 1:
919 Uninduced *E. coli* transformed with nSWD; Line 2: Induced *E. coli* transformed with
920 nSWD; Line 3: Supernatant of ultrasonic lysed *E. coli* expressing nSWD; Line 4:
921 Precipitate of lysed *E. coli* expressing nSWD. Line 5: Purified recombinant nSWD

922 protein (black arrow).

923 **(F)** Western blotting of purified rnSWD protein. Purified rnSWD protein was checked
924 by Western blotting with anti-6×-His Ab.

925 **(G)** Quantity of WSSV copies in shrimp gills following nSWD application post-nSWD
926 knockdown. The quantity of WSSV copies in shrimp gills following 10 μg nSWD
927 application post-nSWD knockdown at high temperature (32 °C) was measured *in vivo*
928 at 24 and 48 hours using absolute quantitative PCR.

929 **(H)** Survival rates post-rnSWD application. Shrimp were injected with 10 μg rnSWD
930 or control protein, mixed with WSSV inoculum post-nSWD knockdown at high
931 temperature (32 °C). Survival rates were recorded every 4 hours.

932 **(I)** Quantity of WSSV copies in shrimp gills following nSWD application post-LvHSF1
933 knockdown. The quantity of WSSV copies in shrimp gills following 10 μg nSWD
934 application post-LvHSF1 knockdown at high temperature (32 °C) was measured *in vivo*
935 at 24 and 48 hours using absolute quantitative PCR.

936 **(J)** Expression of WSSV VP28 protein. Expression of WSSV VP28 protein was
937 detected by Western blotting in gills at high temperature (32 °C) after WSSV infection.
938 Quantification and statistical analysis of three independent repeats were performed
939 using ImageJ (panel j).

940 **(K)** Survival rates post-rnSWD application. Shrimp were injected with 10 μg rnSWD
941 or control protein, mixed with WSSV inoculum post-LvHSF1 knockdown at high
942 temperature (32 °C). Survival rates were recorded every 4 hours.

943 Statistical significance was calculated using the Student's *t*-test (**$p < 0.01$, *$p < 0.05$).
944 All experiments were conducted with three biological replicates, consistently yielding
945 similar results.

946

947 **Figure 7.**

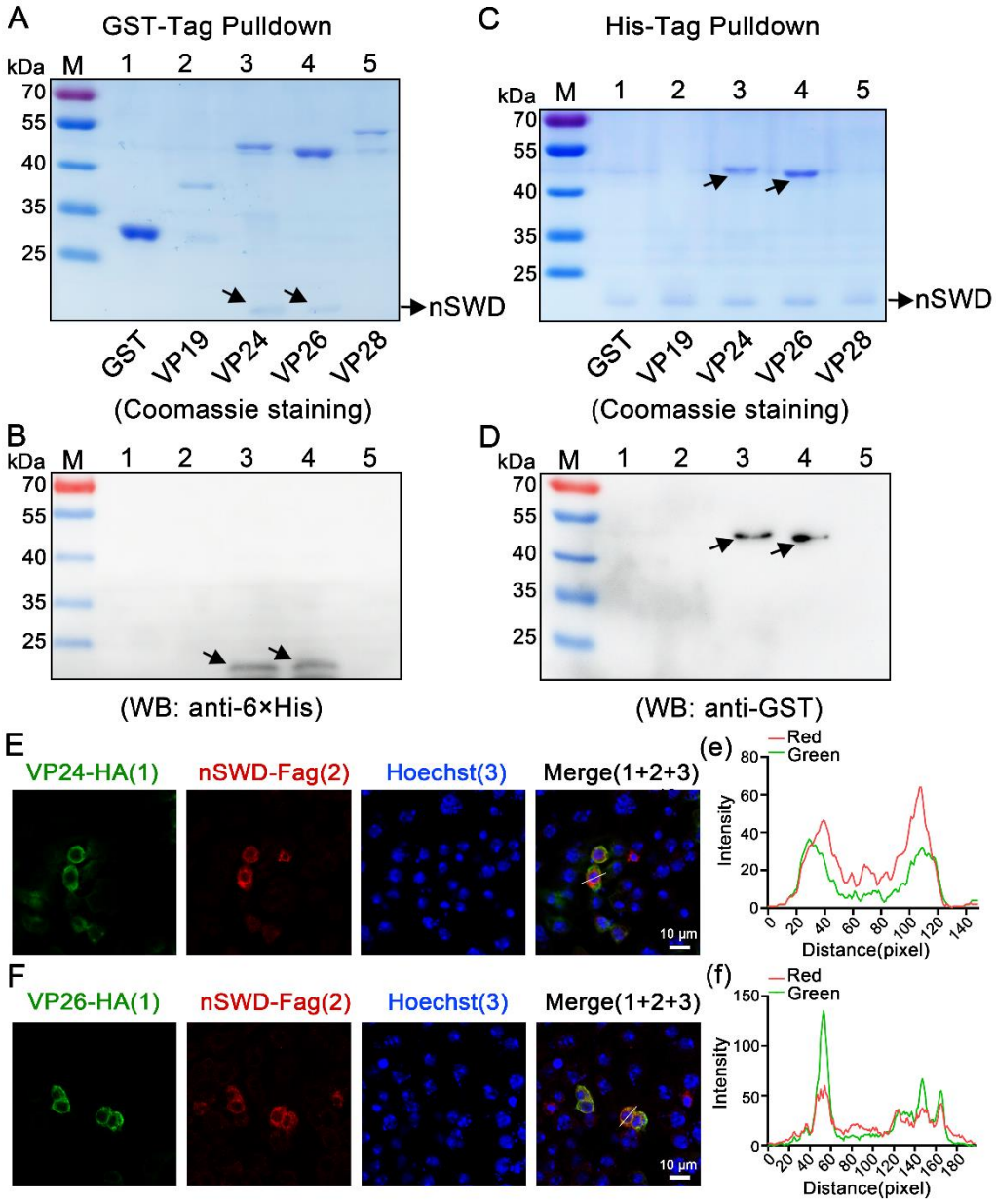

948

949 **Figure 7. nSWD interacts with envelope proteins of WSSV.**

950 **(A, B)** GST pull-down assay for the detection of the interaction between rnSWD with
951 VP19, VP24, VP26, and VP28. The results were shown via staining with Coomassie
952 blue (A) or Western blotting using 6×-His Ab (B). The GST-tag protein was used as a
953 control.

954 **(C, D)** His pull-down assay for the detection of the interaction of rnSWD with VP19,
955 VP24, VP26, and VP28 via Coomassie blue staining (C) or Western blotting using the
956 GST-tag Ab (D). The GST tag protein was used as a control.

957 **(E, F)** The colocalization of nSWD with VP24 and VP26 in S2 cells, 24 hours post-

958 plasmid transfection. VP24 and VP26 was detected with rabbit anti-HA antibodies and
959 anti-rabbit Alexa Fluor 488, while nSWD was identified using anti-Flag antibodies and
960 anti-mouse Alexa Fluor 594. DAPI staining highlighted the nuclei. The scale bar
961 represents 10 μm. (e-f) Quantitative analysis of fluorescence colocalization.
962 Colocalization intensity was quantitatively analyzed, with complete colocalization
963 indicated by overlapping peaks and maxima shifted by less than 20 nm.
964 All experiments were representative of three biological replicates and yielded similar
965 results.
966

967 **Figure 8.**

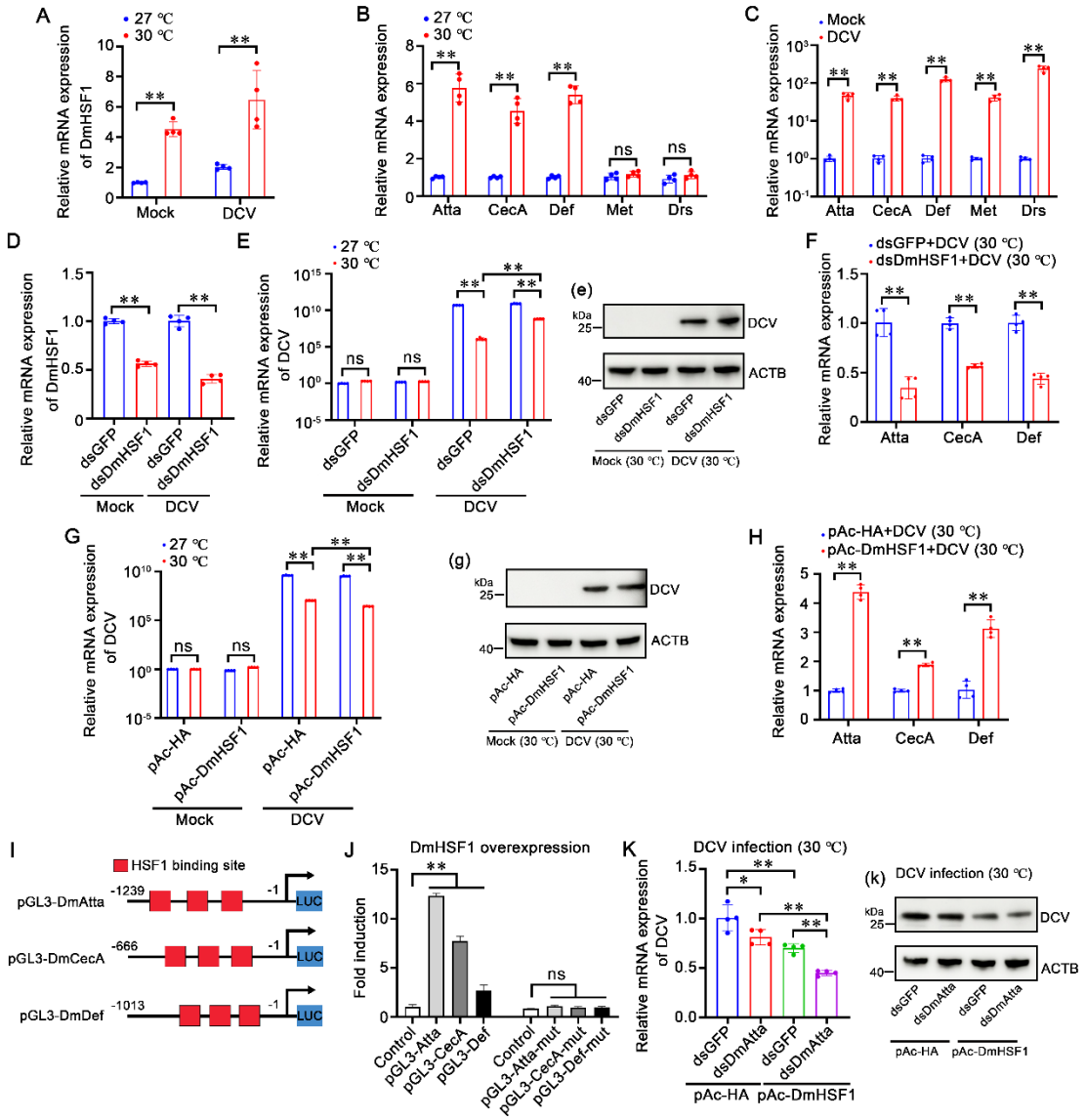

968

969 **Figure 8. High temperature-induced DmHSF1-AMPs axis restricts DCV**
970 **replication in *Drosophila*.**

971 **(A)** Transcriptional expression of DmHSF1. Transcriptional expression of DmHSF1 in
972 S2 cells with or without DCV infection at low (27 °C) and high (30 °C) temperatures.
973 **(B)** Transcriptional expression of DmAMPs. Transcriptional expression of DmAMPs
974 in S2 cells at low (27 °C) and high (30 °C) temperatures.
975 **(C)** Transcriptional expression of DmAMPs with or without DCV infection.
976 Transcriptional expression of DmAMPs in S2 cells with or without DCV infection.
977 **(D)** Silencing efficiency of DmHSF1. Silencing efficiency of DmHSF1 in S2 cells 24
978 hours after dsRNA application with or without DCV infection.

(E) mRNA expression of DCV. mRNA expression of DCV at low (27 °C) and high (30 °C) temperatures after DmHSF1 knockdown, with dsGFP used as a control. (e) Protein expression of DCV at low (27 °C) and high (30 °C) temperatures after DmHSF1 knockdown.

(F) mRNA expression of DmAMPs. mRNA expression of DmAMPs at low (27 °C) and high (30 °C) temperatures after DmHSF1 knockdown and DCV infection.

(G) mRNA expression of DCV after DmHSF1 overexpression. mRNA expression of DCV at low (27 °C) and high (30 °C) temperatures after DmHSF1 overexpression. (g) Protein expression of DCV at low (27 °C) and high (30 °C) temperatures after DmHSF1 overexpression.

(H) mRNA expression of DmAMPs after DmHSF1 overexpression. mRNA expression of DmAMPs at low (27 °C) and high (30 °C) temperatures after DmHSF1 overexpression and DCV infection.

(I) Schematic Diagram of DmAMPs Promoter Regions. Schematic diagram of the DmAMPs promoter regions in the luciferase reporter gene constructs. The HSF1 binding motif sites are shown in red rectangles.

(J) Dual-luciferase reporter assays. Dual-luciferase reporter assays were performed to analyze the effects of DmHSF1 overexpression on the promoter activities of DmAMPs with or without mutated HSF1 binding motifs.

(K) mRNA expression of DCV following DmHSF1 overexpression post-DmAtta Knockdown. mRNA expression of DCV at high (30 °C) temperatures following DmHSF1 overexpression post-DmAtta knockdown. (k) Protein expression of DCV at high (30°C) temperatures following DmHSF1 overexpression post-DmAtta knockdown.

Statistical significance was calculated using the Student's *t*-test (**$p < 0.01$, *$p < 0.05$). All experiments were conducted with three biological replicates, consistently yielding similar results.

1007 **Figure 9.**

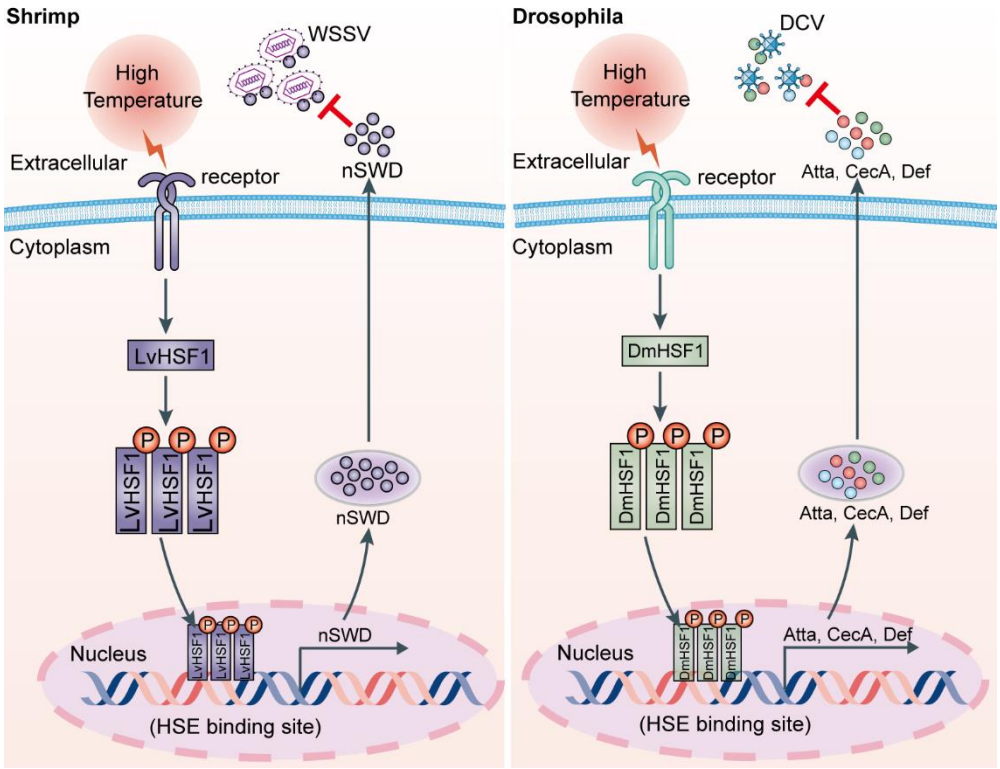

1008

1009 **Figure 9. Model for the HSF1-AMPs-mediated high temperature-induced**
1010 **resistance to viruses in arthropods.**

1011 Elevated temperature induces a robust expression of LvHSF1, which in turn specifically
1012 induces the expression of the antimicrobial peptide (nSWD) in shrimp. The nSWD
1013 directly binds to WSSV envelope proteins and inhibits WSSV replication (**left panel**).
1014 Additionally, elevated temperature induces the expression of DmHSF1, which
1015 upregulates the expression of Atta, CecA, and Def in *Drosophila*, subsequently
1016 restricting the replication of DCV (**right panel**). These findings highlight the roles of
1017 HSF1 beyond the classical heat shock response, mediating the thermal regulation of
1018 immunity and facilitating the innate immune system's response against viruses.

1019

1020

1021

1022

1023

1024

1025 **Supplementary Figure 1. The expression of transcription factors as determined by**

1026 **qPCR.**

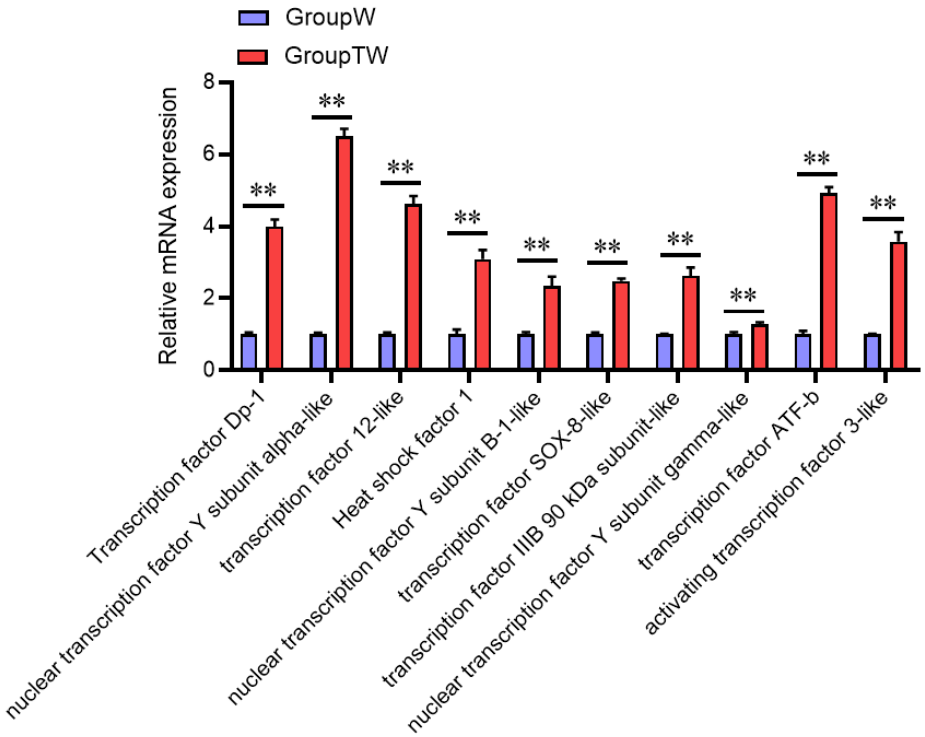

1027

1028

1029 **Supplementary Figure 2. The expression of effector molecules as determined by**

1030 **qPCR.**

1031

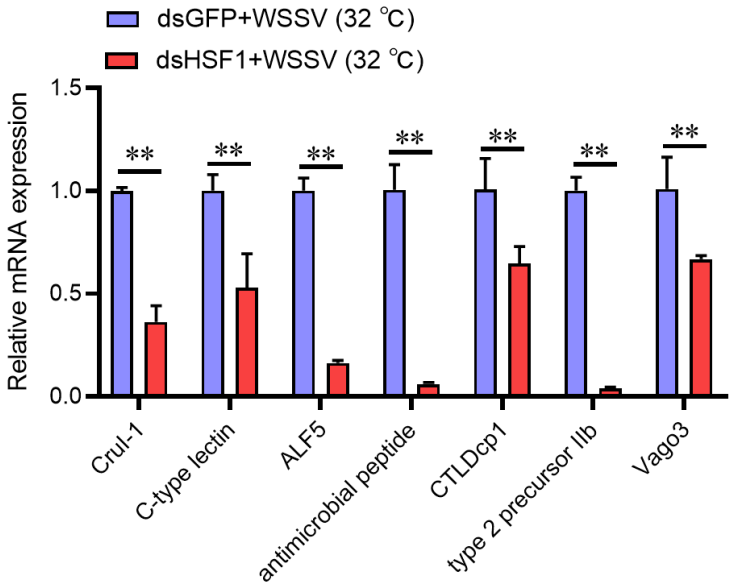

1032

1033 **Supplementary Figure 3. SDS-PAGE and western blotting analyses of the**
1034 **recombinant LvHSF1 protein expressed in *E. coli*.** (A) SDS-PAGE analysis of the
1035 recombinant LvHSF1 protein. Line 1, uninduced *E. coli* transformed with LvHSF1; line
1036 2, induced *E. coli* transformed with LvHSF1; line 3, supernatant of ultrasonic lysed *E.*
1037 *coli* expressing LvHSF1; line 4, precipitate of lysed *E. coli* expressing LvHSF1; line 5,
1038 purified recombinant LvHSF1 protein (black arrow). (B) Western blotting analysis of
1039 the recombinant LvHSF1 protein. Line 1, rLvHSF1-GST; Line 2, GST (black arrow).
1040 Purified proteins were checked by Western blotting with anti-GST.
1041

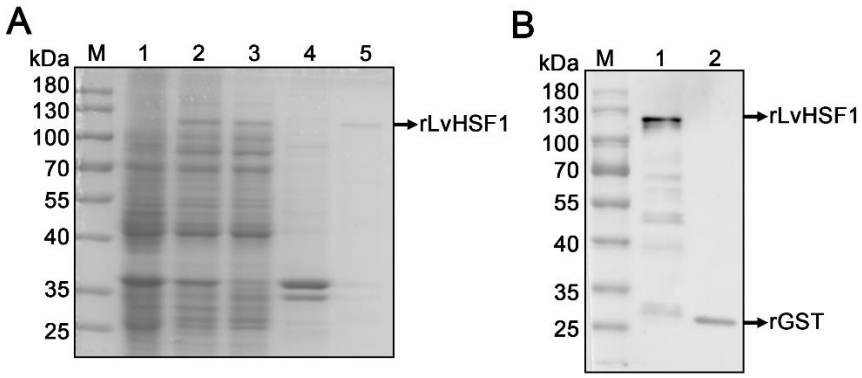

1042
1043

1044 **Supplementary Figure 4. High temperature restricts DCV replication in**
1045 ***Drosophila* S2 cells.** (A) *Drosophila* S2 cells were seeded in 6-well plate and incubated
1046 at 27 ℃ or 30 ℃ for 24 h, then the cells were infected with DCV at a multiplicity of
1047 infection (MOI) of 10 at 27 ℃ or 30 ℃ for another 24 h. The cytopathic signs of S2
1048 cells were observed in inverted fluorescence microscope. (B) The transcriptional
1049 expression of DCV in S2 cells with or without DCV infection (black arrow). (C) The
1050 protein expression of DCV in S2 cells with or without DCV infection.
1051

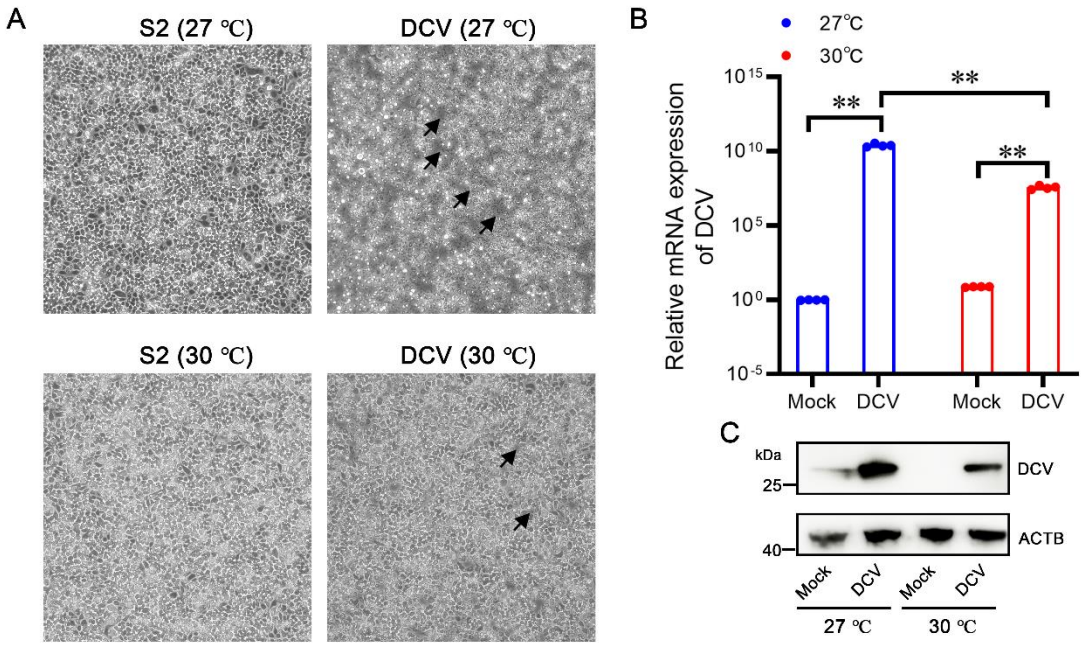

1052

1053

1054 **Supplementary Figure 5. Transfection in S2 cells.** (A) The protein expression level

1055 of DmHSF1 was detected by western blotting at 48 h post-transfection in S2 cells. (B)

1056 The silencing efficiency of DmAtta in S2 cells 24 h after dsRNA application with or

1057 without DCV infection.

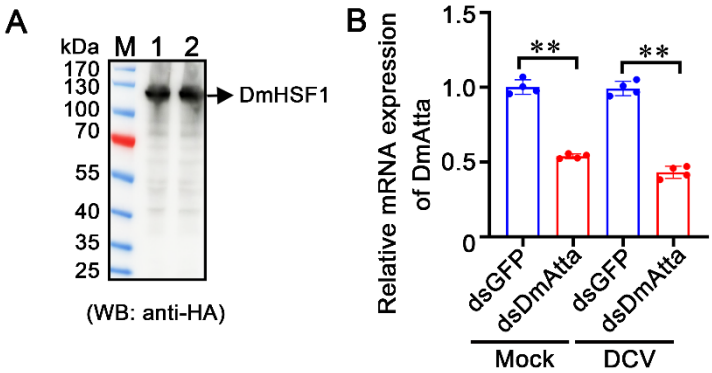

1058

1059

1060 **Reference**

1061 Akerfelt, M., Morimoto, R.I., Sistonen, L., 2010. Heat shock factors: integrators of cell stress,
1062 development and lifespan. Nat Rev Mol Cell Biol 11, 545-555.
1063 Akerfelt, M., Trouillet, D., Mezger, V., Sistonen, L., 2007. Heat shock factors at a crossroad between stress
1064 and development. Ann N Y Acad Sci 1113, 15-27.
1065 Amin, J., Ananthan, J., Voellmy, R., 1988. Key features of heat shock regulatory elements. Mol Cell Biol
1066 8, 3761-3769.
1067 Anckar, J., Sistonen, L., 2011. Regulation of HSF1 function in the heat stress response: implications in
1068 aging and disease. Annu Rev Biochem 80, 1089-1115.
1069 Barna, J., Csermely, P., Vellai, T., 2018. Roles of heat shock factor 1 beyond the heat shock response. Cell
1070 Mol Life Sci 75, 2897-2916.
1071 Bicego, K.C., Barros, R.C.H., Branco, L.G.S., 2007. Physiology of temperature regulation: comparative
1072 aspects. Comp Biochem Physiol A Mol Integr Physiol 147, 616-639.
1073 Brogden, K.A., 2005. Antimicrobial peptides: pore formers or metabolic inhibitors in bacteria? Nat Rev
1074 Microbiol 3, 238-250.
1075 Bundey, S., Raymond, S., Dean, P., Roberts, S.K., Dillon, R.J., Charnley, A.K., 2003. Eicosanoid involvement
1076 in the regulation of behavioral fever in the desert locust, Schistocerca gregaria. Arch Insect Biochem
1077 Physiol 52, 183-192.
1078 Carpenter, S., O'Neill, L.A.J., 2024. From periphery to center stage: 50 years of advancements in innate
1079 immunity. Cell 187, 2030-2051.
1080 Casterlin, M.E., Reynolds, W.W., 1978. Prostaglandin E1 fever in the crayfish Cambarus bartoni.
1081 Pharmacol Biochem Behav 9, 593-595.
1082 Casterlin, M.E., Reynolds, W.W., 1979. Fever induced in marine arthropods by prostaglandin E1. Life Sci
1083 25, 1601-1603.
1084 Chen, J., Xie, C., Tian, L., Hong, L., Wu, X., Han, J., 2010. Participation of the p38 pathway in Drosophila
1085 host defense against pathogenic bacteria and fungi. Proc Natl Acad Sci U S A 107, 20774-20779.
1086 Covert, J.B., Reynolds, W.W., 1977. Survival value of fever in fish. Nature 267, 43-45.
1087 Deldicq, N., Langlet, D., Delaeter, C., Beaugrand, G., Seuront, L., Bouchet, V.M.P., 2021. Effects of
1088 temperature on the behaviour and metabolism of an intertidal foraminifera and consequences for
1089 benthic ecosystem functioning. Sci Rep 11, 4013.
1090 Du, H.H., Li, W.F., Xu, Z.R., Kil, Z.S., 2006. Effect of hyperthermia on the replication of white spot
1091 syndrome virus (WSSV) in Procambarus clarkii. Dis Aquat Organ 71, 175-178.
1092 Evans, S.S., Repasky, E.A., Fisher, D.T., 2015. Fever and the thermal regulation of immunity: the immune
1093 system feels the heat. Nat Rev Immunol 15, 335-349.
1094 Fan-xin, M., Li-mei, S., Bei, S., Xin, Q., Yu, Y., Yu, C., 2012. Heat shock factor 1 regulates the expression
1095 of the TRPV1 gene in the rat preoptic-anterior hypothalamus area during lipopolysaccharide-induced
1096 fever. Exp Physiol 97, 730-740.
1097 Filone, C.M., Caballero, I.S., Dower, K., Mendillo, M.L., Cowley, G.S., Santagata, S., Rozelle, D.K., Yen, J.,
1098 Rubins, K.H., Hacohen, N., Root, D.E., Hensley, L.E., Connor, J., 2014. The master regulator of the cellular
1099 stress response (HSF1) is critical for orthopoxvirus infection. PLoS Pathog 10, e1003904.
1100 Freitas Lione, V.O., Bittencourt Dos Santos, M.H., Ulisses Carvalho, T.M., Hirata, R., Jr., Mattos-Guaraldi,
1101 A.L., Arruda Mortara, R., Nagao, P.E., 2010. Fever temperature enhances mechanisms of survival of
1102 Streptococcus agalactiae within human endothelial cells. Int J Mol Med 26, 511-516.
1103 Fu, Q., Li, H., Wang, S., Liao, X., Chen, S., Xiao, B., Chen, R., Jiang, X., He, J., Li, C., 2022. An AhR-Caspase

1104 Axis Mediated Antiviral Apoptosis in an Arthropod. J Immunol 209, 2022-2032.
1105 Granja, C.B., Aranguren, L.F., Vidal, O.M., Aragon, L., Salazar, M., 2003. Does hyperthermia increase
1106 apoptosis in white spot syndrome virus (WSSV)-infected Litopenaeus vannamei? Dis Aquat Organ 54,
1107 73-78.
1108 Guan, Y., Yu, Z., Li, C., 2003. The effects of temperature on white spot syndrome infections in
1109 Marsupenaeus japonicus. J Invertebr Pathol 83, 257-260.
1110 Hahn, J.S., Hu, Z., Thiele, D.J., Iyer, V.R., 2004. Genome-wide analysis of the biology of stress responses
1111 through heat shock transcription factor. Mol Cell Biol 24, 5249-5256.
1112 Hasday, J.D., Singh, I.S., 2000. Fever and the heat shock response: distinct, partially overlapping
1113 processes. Cell Stress Chaperones 5, 471-480.
1114 Hasday, J.D., Thompson, C., Singh, I.S., 2014. Fever, immunity, and molecular adaptations. Compr Physiol
1115 4, 109-148.
1116 Hou, G., Lv, Z., Liu, W., Xiong, S., Zhang, Q., Li, C., Wang, X., Hu, L., Ding, C., Song, R., Wang, H., Zhang,
1117 Y.A., Xiao, T., Li, J., 2023. An aquatic virus exploits the IL6-STAT3-HSP90 signaling axis to promote viral
1118 entry. PLoS Pathog 19, e1011320.
1119 Jiravanichpaisal, P., Soderhall, K., Soderhall, I., 2004. Effect of water temperature on the immune
1120 response and infectivity pattern of white spot syndrome virus (WSSV) in freshwater crayfish. Fish
1121 Shellfish Immunol 17, 265-275.
1122 Kluger, M.J., Ringler, D.H., Anver, M.R., 1975. Fever and survival. Science 188, 166-168.
1123 Li, H., Di, X., Wang, S., Li, Q., Weng, S., He, J., Li, C., 2024. Nucleic Acid Sensing by STING Induces an IFN-
1124 like Antiviral Response in a Marine Invertebrate. J Immunol.
1125 Li, H., Yin, B., Wang, S., Fu, Q., Xiao, B., Lu, K., He, J., Li, C., 2018. RNAi screening identifies a new Toll
1126 from shrimp Litopenaeus vannamei that restricts WSSV infection through activating Dorsal to induce
1127 antimicrobial peptides. PLoS Pathog 14, e1007109.
1128 Li, Z., Chen, W., Xu, L., Li, F., Yang, F., 2015. Identification of the interaction domains of white spot
1129 syndrome virus envelope proteins VP28 and VP24. Virus Res 200, 24-29.
1130 Lin, Y.R., Hung, H.C., Leu, J.H., Wang, H.C., Kou, G.H., Lo, C.F., 2011. The role of aldehyde dehydrogenase
1131 and hsp70 in suppression of white spot syndrome virus replication at high temperature. J Virol 85, 3517-
1132 3525.
1133 Liu, L.K., Jian, J.T., Jing, S.S., Gao, R.L., Chi, X.D., Tian, G., Liu, H.P., 2024. The crustacean DNA virus
1134 tegument protein VP26 binds to SNAP29 to inhibit SNARE complex assembly and autophagic
1135 degradation. J Virol 98, e0140823.
1136 Loh, E., Kugelberg, E., Tracy, A., Zhang, Q., Gollan, B., Ewles, H., Chalmers, R., Pelicic, V., Tang, C.M., 2013.
1137 Temperature triggers immune evasion by Neisseria meningitidis. Nature 502, 237-240.
1138 Louis, C., Jourdan, M., Cabanac, M., 1986. Behavioral fever and therapy in a rickettsia-infected
1139 Orthoptera. Am J Physiol 250, R991-995.
1140 M.E. Casterlin, W.W.R., 1977. Bahavioral fever in crayfish. Hydrobiologia 56, 99-101.
1141 Marcogliese, D.J., 2008. The impact of climate change on the parasites and infectious diseases of aquatic
1142 animals. Rev Sci Tech 27, 467-484.
1143 Matos, G.M., Rosa, R.D., 2022. On the silver jubilee of crustacean antimicrobial peptides. Rev Aquacult
1144 14, 594-612.
1145 Merkling, S.H., Overheul, G.J., van Mierlo, J.T., Arends, D., Gilissen, C., van Rij, R.P., 2015. The heat shock
1146 response restricts virus infection in Drosophila. Sci Rep 5, 12758.
1147 Millard, R.S., Ellis, R.P., Bateman, K.S., Bickley, L.K., Tyler, C.R., van Aerle, R., Santos, E.M., 2021. How do

1148 abiotic environmental conditions influence shrimp susceptibility to disease? A critical analysis focussed
1149 on White Spot Disease. J Invertebr Pathol 186, 107369.
1150 Morano, K.A., Grant, C.M., Moye-Rowley, W.S., 2012. The response to heat shock and oxidative stress
1151 in Saccharomyces cerevisiae. Genetics 190, 1157-1195.
1152 Morimoto, R.I., 2011. The heat shock response: systems biology of proteotoxic stress in aging and
1153 disease. Cold Spring Harb Symp Quant Biol 76, 91-99.
1154 Neef, D.W., Jaeger, A.M., Gomez-Pastor, R., Willmund, F., Frydman, J., Thiele, D.J., 2014. A direct
1155 regulatory interaction between chaperonin TRiC and stress-responsive transcription factor HSF1. Cell
1156 Rep 9, 955-966.
1157 Nekongo, E.E., Ponomarenko, A.I., Dewal, M.B., Butty, V.L., Browne, E.P., Shoulders, M.D., 2020. HSF1
1158 Activation Can Restrict HIV Replication. ACS Infect Dis 6, 1659-1666.
1159 Niu, G.J., Wang, S., Xu, J.D., Yang, M.C., Sun, J.J., He, Z.H., Zhao, X.F., Wang, J.X., 2019. The polymeric
1160 immunoglobulin receptor-like protein from Marsupenaeus japonicus is a receptor for white spot
1161 syndrome virus infection. PLoS Pathog 15, e1007558.
1162 Pan, X.Y., Zhao, W., Zeng, X.Y., Lin, J., Li, M.M., Shen, X.T., Liu, S.W., 2016. Heat Shock Factor 1 Mediates
1163 Latent HIV Reactivation. Sci Rep 6, 26294.
1164 Rahman, M.M., Corteel, M., Wille, M., Alday-Sanz, V., Pensaert, M.B., Sorgeloos, P., Nauwynck, H.J.,
1165 2007. The effect of raising water temperature to 33 °C in Penaeus vannamei juveniles at different stages
1166 of infection with white spot syndrome virus (WSSV). Aquaculture 272, 240-245.
1167 Rakhshaninejad, M., Zheng, L., Nauwynck, H., 2023. Shrimp (Penaeus vannamei) survive white spot
1168 syndrome virus infection by behavioral fever. Sci Rep 13, 18034.
1169 Rakus, K., Ronsmans, M., Forlenza, M., Boutier, M., Piazzon, M.C., Jazowiecka-Rakus, J., Gatherer, D.,
1170 Athanasiadis, A., Farnir, F., Davison, A.J., Boudinot, P., Michiels, T., Wiegertjes, G.F., Vanderplasschen, A.,
1171 2017. Conserved Fever Pathways across Vertebrates: A Herpesvirus Expressed Decoy TNF-alpha
1172 Receptor Delays Behavioral Fever in Fish. Cell Host Microbe 21, 244-253.
1173 Reyes, A., Navarro, A.J., Diethelm-Varela, B., Kalergis, A.M., Gonzalez, P.A., 2022. Is there a role for HSF1
1174 in viral infections? FEBS Open Bio 12, 1112-1124.
1175 Singh, V., Aballay, A., 2006. Heat-shock transcription factor (HSF)-1 pathway required for Caenorhabditis
1176 elegans immunity. Proc Natl Acad Sci U S A 103, 13092-13097.
1177 Sun, Y., Li, F., Sun, Z., Zhang, X., Li, S., Zhang, C., Xiang, J., 2014. Transcriptome analysis of the initial stage
1178 of acute WSSV infection caused by temperature change. PLoS One 9, e90732.
1179 Wang, S., Li, H., Weng, S., Li, C., He, J., 2020. White Spot Syndrome Virus Establishes a Novel IE1/JNK/c-
1180 Jun Positive Feedback Loop to Drive Replication. iScience 23, 100752.
1181 Wang, S., Sun, Y., Wang, Y., Wang, A., Kou, B., Che, Y., Chen, D., Zhang, Y., Shi, Y., 2021. ASPP2 inhibits
1182 hepatitis B virus replication by preventing nucleus translocation of HSF1 and attenuating the
1183 transactivation of ATG7. J Cell Mol Med 25, 6899-6908.
1184 Wang, X.X., Zhang, H., Gao, J., Wang, X.W., 2024. Ammonia stress-induced heat shock factor 1 enhances
1185 white spot syndrome virus infection by targeting the interferon-like system in shrimp. mBio 15,
1186 e0313623.
1187 Weihrauch, D., Joseph, G., Allen, G.J.P., 2018. Ammonia excretion in aquatic invertebrates: new insights
1188 and questions. J Exp Biol 221.
1189 Wu, X., Xiong, H., Wang, Y., Du, H., 2015. Immunomodulatory effects of hyperthermia on resisting WSSV
1190 infection in Procambarus clarkii. J Fish Dis 38, 567-574.
1191 Xiao, B., Fu, Q., Niu, S., Zhu, P., He, J., Li, C., 2020. Penaeidins restrict white spot syndrome virus infection

1192 by antagonizing the envelope proteins to block viral entry. Emerg Microbes Infect 9, 390-412.
1193 Xiao, B., Liao, X., Wang, H., He, J., Li, C., 2021. BigPEN, an antimicrobial peptide of penaeidin family from
1194 shrimp Litopenaeus vannamei with membrane permeable and DNA binding activity. Fish Shellfish
1195 Immunol Rep 2, 100034.
1196 Xiao, H., Lis, J.T., 1988. Germline transformation used to define key features of heat-shock response
1197 elements. Science 239, 1139-1142.
1198 Yang, S., Yu, J., Fan, Z., Gong, S.T., Tang, H., Pan, L., 2018. Bub1 Facilitates Virus Entry through Endocytosis
1199 in a Model of Drosophila Pathogenesis. J Virol 92.
1200 You, X.X., Su, Y.Q., Mao, Y., Liu, M., Wang, J., Zhang, M., Wu, C., 2010. Effect of high water temperature
1201 on mortality, immune response and viral replication of WSSV-infected
1202 juveniles and adults. Aquaculture 305, 133-137.
1203 Yuasa, K., Ito, T., Sano, M., 2008. Effect of Water Temperature on Mortality and Virus Shedding in Carp
1204 Experimentally Infected with Koi Herpesvirus. Fish Pathol 43, 83-85.
1205 Zhang, X., Yuan, J., Sun, Y., Li, S., Gao, Y., Yu, Y., Liu, C., Wang, Q., Lv, X., Zhang, X., Ma, K.Y., Wang, X., Lin,
1206 W., Wang, L., Zhu, X., Zhang, C., Zhang, J., Jin, S., Yu, K., Kong, J., Xu, P., Chen, J., Zhang, H., Sorgeloos, P.,
1207 Sagi, A., Alcivar-Warren, A., Liu, Z., Wang, L., Ruan, J., Chu, K.H., Liu, B., Li, F., Xiang, J., 2019. Penaeid
1208 shrimp genome provides insights into benthic adaptation and frequent molting. Nat Commun 10, 356.
1209 Zheng, X., Krakowiak, J., Patel, N., Beyzavi, A., Ezike, J., Khalil, A.S., Pincus, D., 2016. Dynamic control of
1210 Hsf1 during heat shock by a chaperone switch and phosphorylation. Elife 5.
1211 Zou, J., Guo, Y., Guettouche, T., Smith, D.F., Voellmy, R., 1998. Repression of heat shock transcription
1212 factor HSF1 activation by HSP90 (HSP90 complex) that forms a stress-sensitive complex with HSF1. Cell
1213 94, 471-480.
1214